Computational Modeling of Gas-Particle Flows in Rotorcraft Icing and Planetary Landings

October 31st (Tue), 2023

Rho Shin Myong

Professor, School of Aerospace and Software Engineering
Director, Engineering Research Center for Aircraft Core Technology
Leader, Mega Project for Hydrogen Fuel Cell Commuter Aircraft
Gyeongsang National University (GNU)
Jinju, Republic of Korea
myong@gnu.ac.kr

Presented at 14th Asian Computational Fluid Dynamics Conference (ACFD 2023), Bengaluru, India

ACT
Research Center for Aircraft Core Technology

GNU
경상국립대학교
Gyeongsang National University

Linchpin technology and computational modeling

Linchpin technology

Linchpin (the pin going through the axle of a wheel to keep it in place) means a small piece, but everything collapses without it.

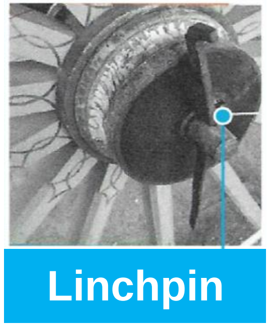

Rotorcraft icing on Earth and planetary landings in outer space are characterized by the **two-phase flow** of compressible air-droplet and gas-particle, respectively.

Computational modeling of these flows is challenging due to large variations in temperature, particle concentration, including the near-zero limit, and flow velocity, as well as the complexities and nonlinearities of the flow involved in rotorcraft with rotor blades and planetary landers with rocket motors.

Computational modeling is the process of using mathematical equations and computational methods to simulate and predict the behavior of complex systems.

Numerical analysis, on the other hand, is the study of algorithms and methods for solving mathematical problems numerically.

Acknowledgements

Organizers of ACFD 2023

Ass. Prof. Hakjin Lee (Gyeongsang National University, Republic of Korea)

Dr. Bidesh Sengupta (NTU, Singapore)

Dr. Omid Ejtehadi (University of Edinburgh, UK)

Ass. Prof. Tapan K. Mankodi (IIT Guwahati, India)

Ass. Prof. L. Prince Raj (IIEST Shibpur, India)

In-flight icing: a critical safety issue

- Icing is an atmospheric phenomenon which deserves adequate protection of aircraft.
- Icing is a **key certification issue** related to **aircraft safety.**
- Need to predict **most critical icing conditions** and the resulting ice shapes within the flight and certification envelopes.
- **Anti-icing** systems: **Prevent** the ice from forming/adhering
- **De-icing** systems: **Remove** the accumulated ice before incurring significant aerodynamic penalties

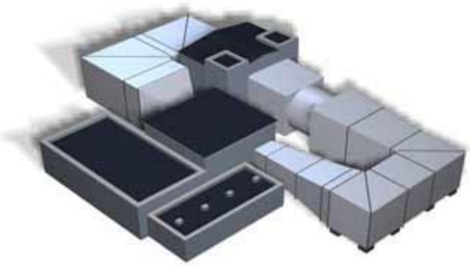

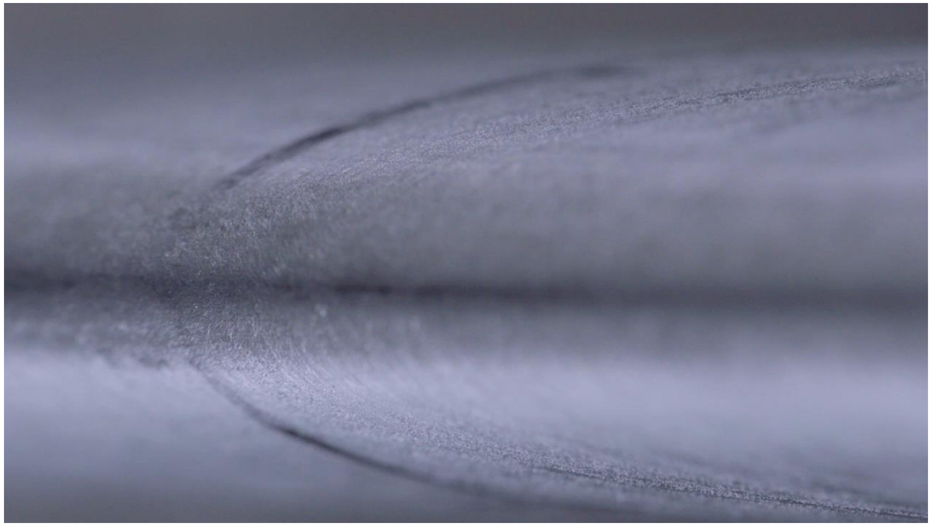

Icing parameters (meteorological/physical/modeling)

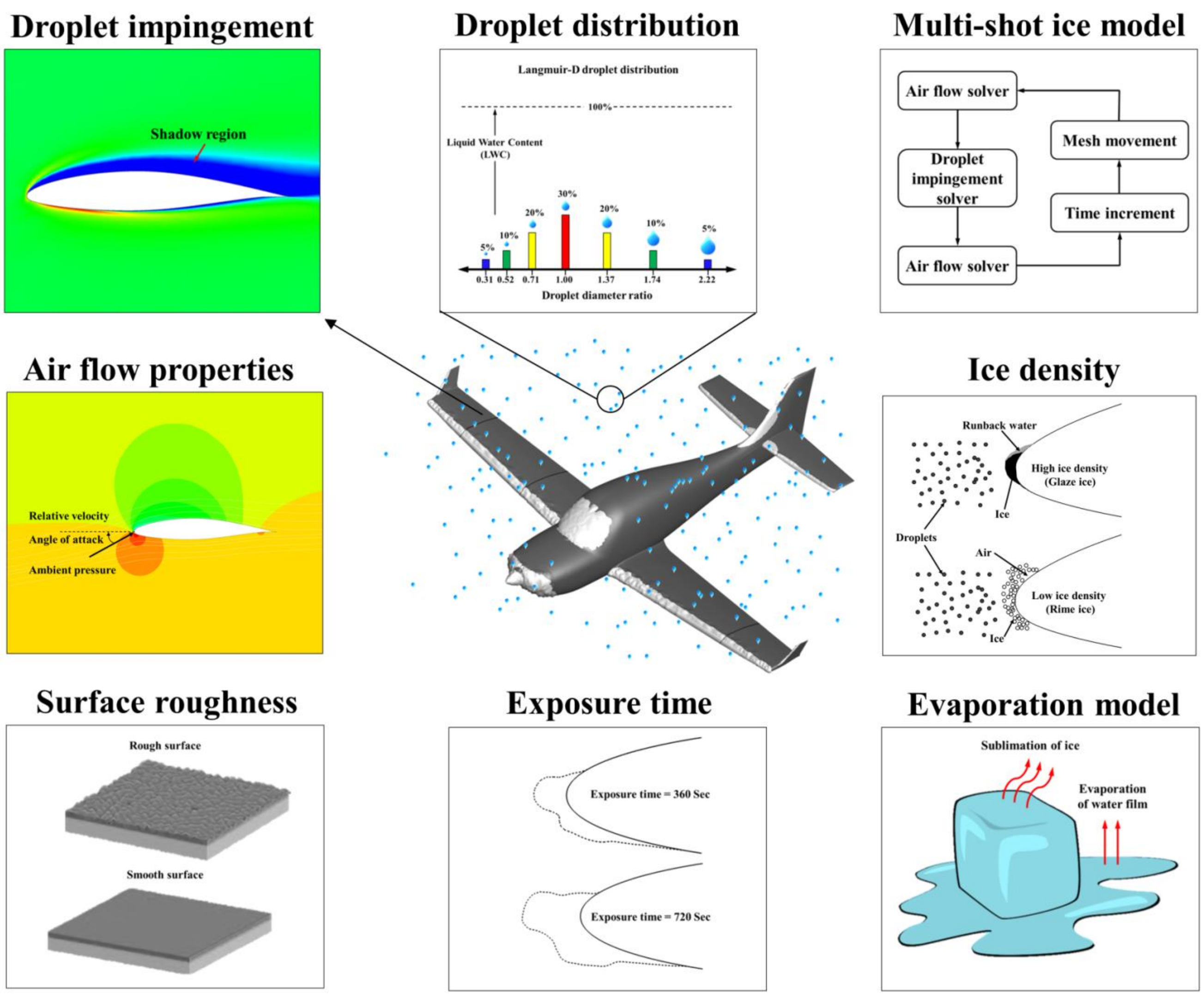

Atmospheric ice accretion depends on

Point of operation (location & altitude etc.)

Geometry of aircraft

Relative **velocity**
Atmospheric **temperature**
Droplet diameter **size**
Liquid water content

Prince Raj, L., Yee, K., Myong, R. S. "Sensitivity of critical parameters affecting ice accretion shape and performance degradation in aircraft wing icing," *Aerospace Science and Technology*, Vol. 98, 105659, 2020.

Aircraft in-flight icing: IPS (Ice Protection System)

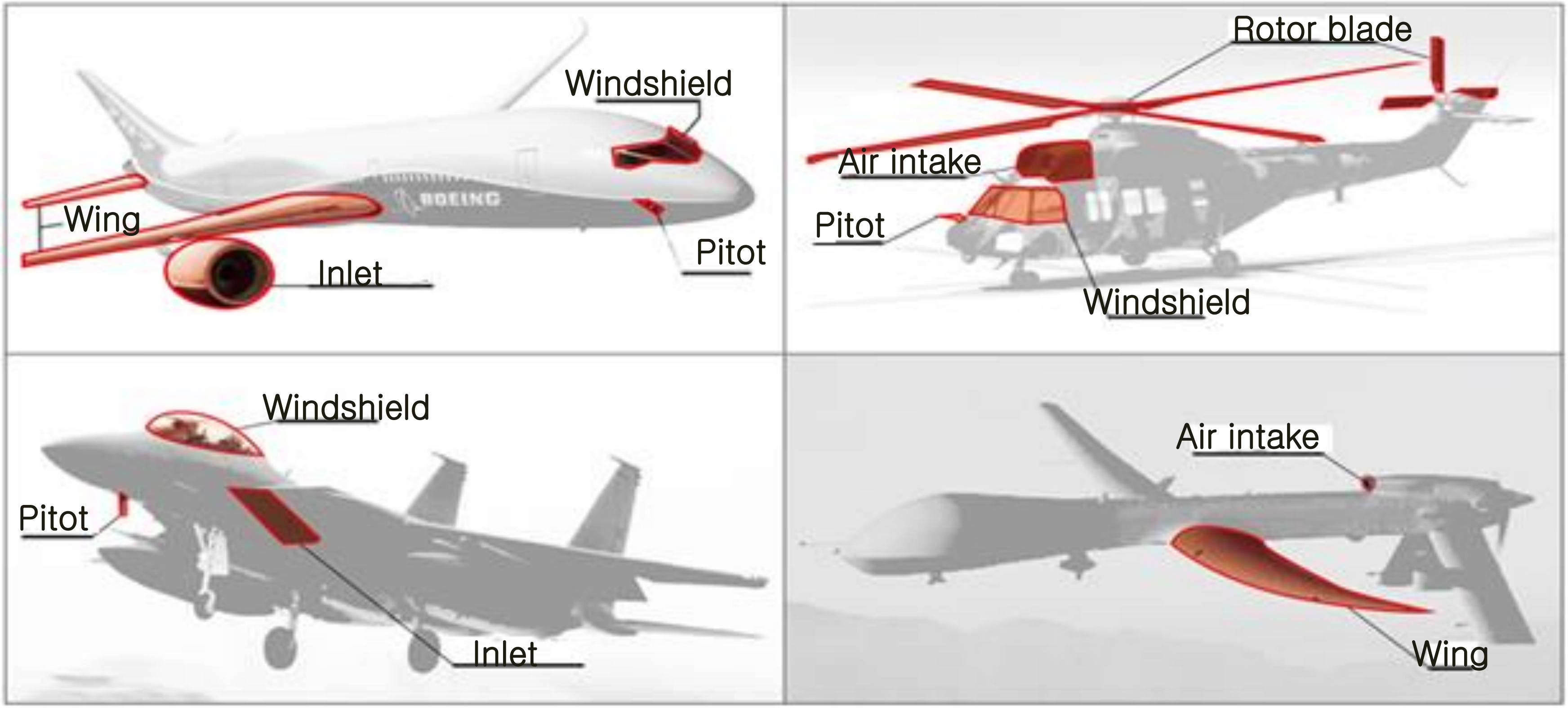

Hot air

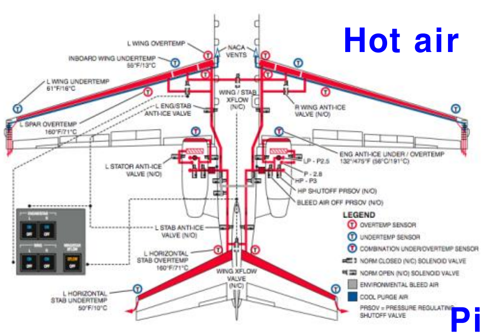

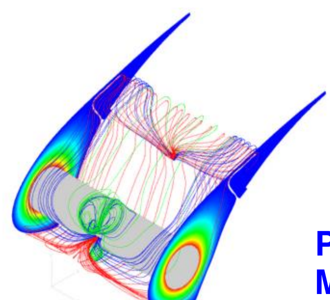

Piccolo tube

Heat mat

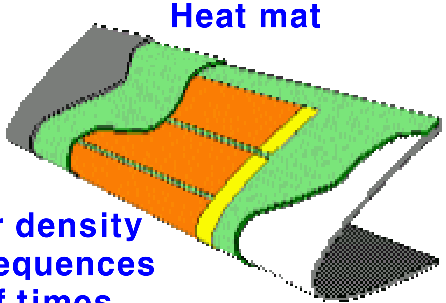

Power density
Mat sequences
On/off times

Impulse

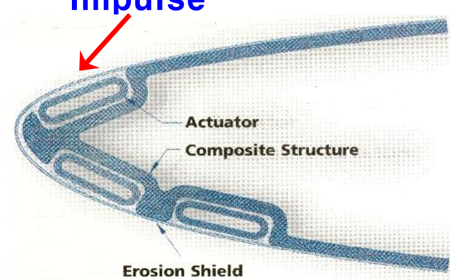

Korean Utility Helicopter program 2015-2018

(Korean) Utility Helicopter Surion 'Failed' at Platform-Level Icing Certification

Icing certification campaign: failure & 2nd full effort

A critical redesign of IPS

More than 130g for 2 minutes

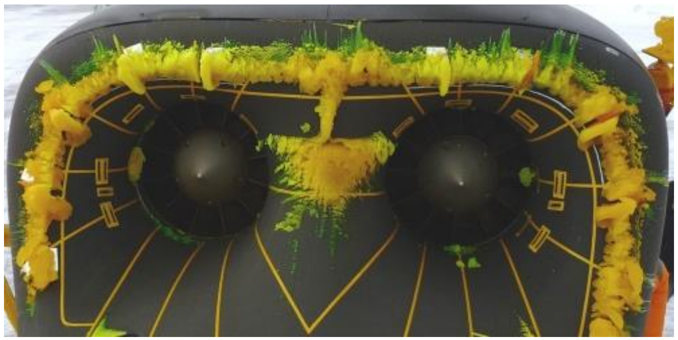

Season 2015-16

Removing runback ice

Higher surface temperature
More time for evaporation
Longer distance for evaporation

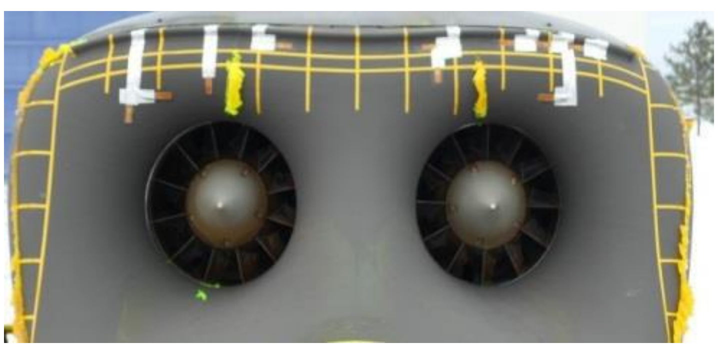

Season 2017-18

Clearance of ice shedding of windshield & wiper

Season 2017-18

Courtesy of Korea Aerospace Industries LTD (KAI) (2018)

Icing computational simulation

- Validation of icing CFD (FENSAP-ICE) prediction (heat-off mode)

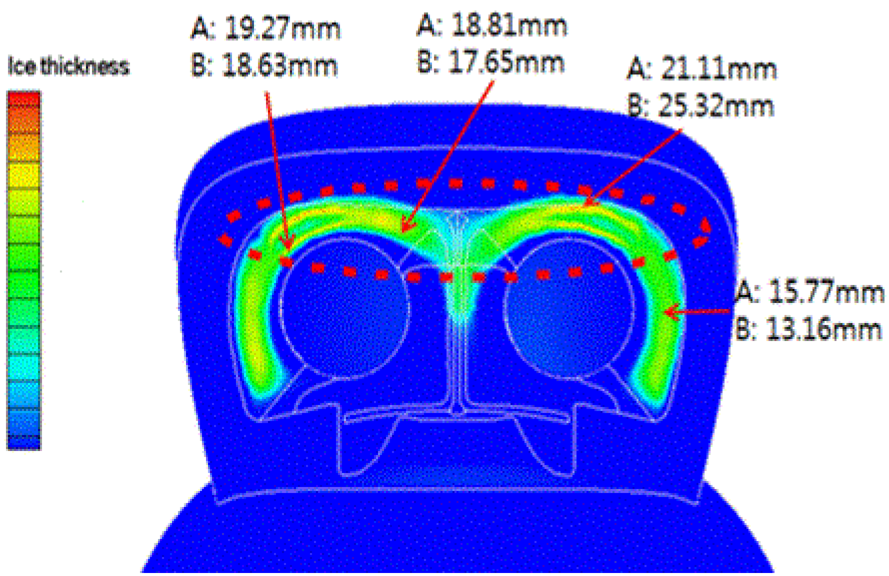

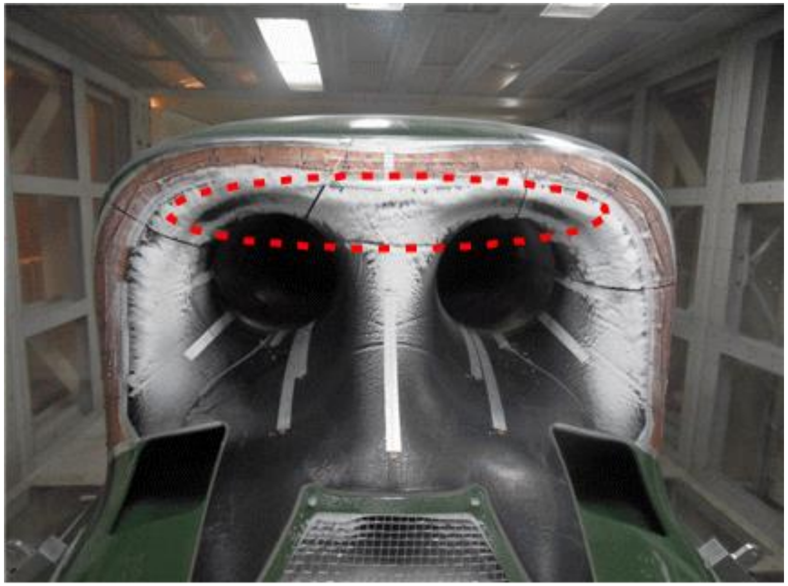

The upper parts of intake with largest ice accretion.
Narrow region with small ice accretion between these parts.

Ahn, G. B., Jung, K. Y., Myong, R. S., Shin, H. B., Habashi, W. G., "Numerical and experimental investigation of ice accretion on a rotorcraft engine air intake," *Journal of Aircraft*, Vol. 52, No. 3, pp. 903-909, 2015.

Flow field of a rotorcraft and ice break-off

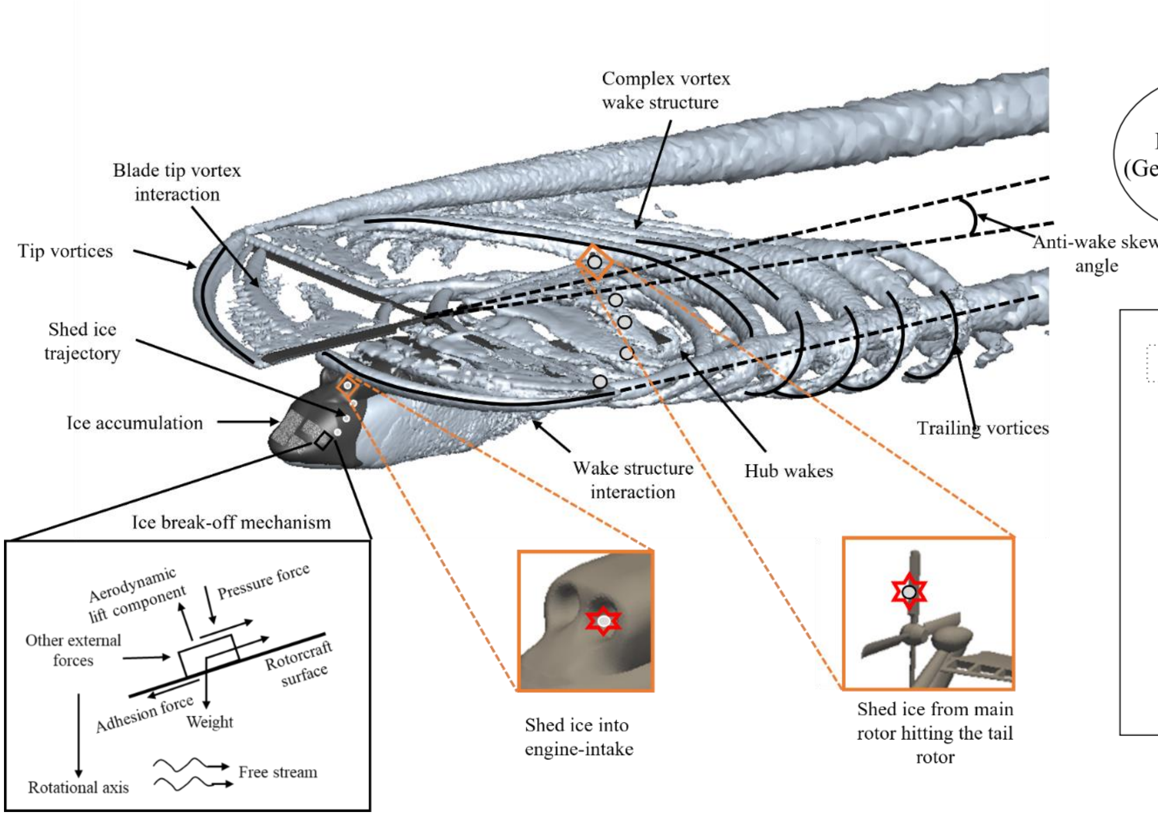

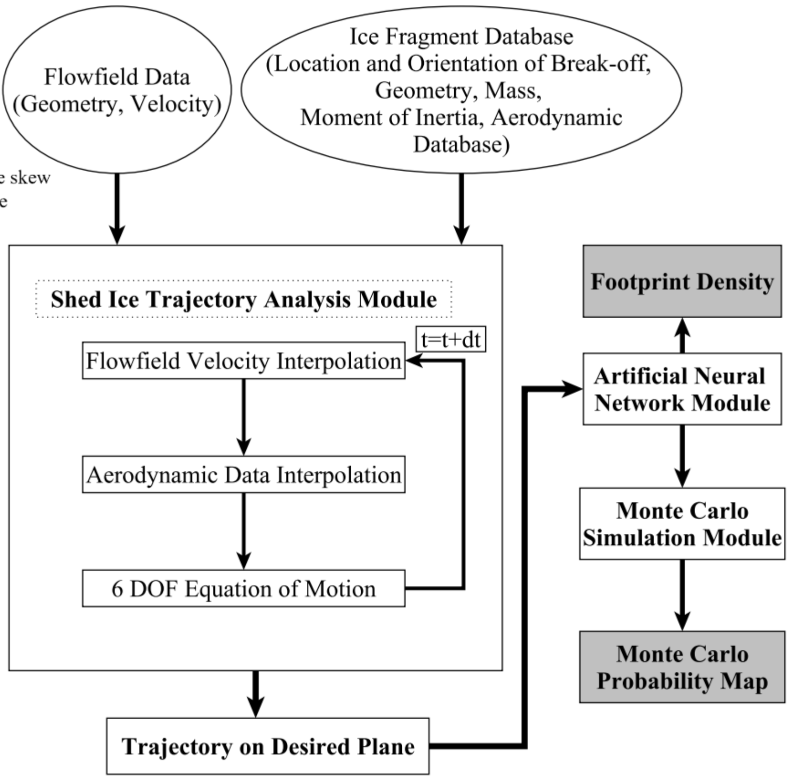

Sengupta, B., Prince Raj, L., Cho, M. Y., Son, C., Yoon, T., Yee, K., Myong, R. S., "Computational Simulation of Ice Accretion and Shedding Trajectory of a Rotorcraft in Forward Flight with Strong Rotor Wakes," *Aerospace Science and Technology*, Vol. 119, 107140, 2021.

CFD-FVM methods base on multi-disciplinary physics

Equations for clean air

$$\begin{bmatrix}\rho_g\\ \rho_g\mathbf{u}_g\\ E\end{bmatrix}_t+\nabla\cdot\begin{bmatrix}\rho_g\mathbf{u}_g\\ \rho_g\mathbf{u}_g\mathbf{u}_g+p\mathbf{I}\\ (E+p)\mathbf{u}_g\end{bmatrix}=\nabla\cdot\begin{bmatrix}0\\ \boldsymbol{\tau}\\ \boldsymbol{\tau}\cdot\mathbf{u}_g+\mathbf{Q}\end{bmatrix},\quad \begin{array}{l}\boldsymbol{\tau}=2\mu\left[\nabla\mathbf{u}_g\right]^{(2)}\\ \mathbf{Q}=k\nabla T\end{array}$$

Shear stress
Heat flux

Equations for droplets

$$\begin{bmatrix}\rho\\ \rho\mathbf{u}\end{bmatrix}_t+\nabla\cdot\begin{bmatrix}\rho\mathbf{u}\\ \rho\mathbf{u}\mathbf{u}+\rho\mathbf{g}d\mathbf{I}\end{bmatrix}=\begin{bmatrix}0\\ \mathbf{S}_D+\mathbf{S}_G+\mathbf{S}_S\end{bmatrix}$$

Droplet impact velocity
Collection efficiency

Equations for ice accretion

$$\begin{bmatrix}h_f\\ h_f T_{equi}\end{bmatrix}_t+\nabla\cdot\begin{bmatrix}\dfrac{h_f^2}{2\mu_w}\tau_{wall}\\ \dfrac{h_f^2 T_{equi}}{2\mu_w}\tau_{wall}\end{bmatrix}=\begin{bmatrix}\dfrac{S_M}{\rho_w}\\ \dfrac{S_E}{\rho_w Cp_{,w}}+\dfrac{T_c S_M}{\rho_w}\end{bmatrix}$$

$$S_M=U_\infty LWC_\infty\beta-\dot{m}_{evap}-\dot{m}_{ice}$$

$$S_E=\left[Cp_{,w}\tilde{T}_{d,\infty}+\frac{\left\|\vec{u}_d\right\|^2}{2}\right]\times U_\infty LWC_\infty\beta-L_{evap}\dot{m}_{evap}$$

$$+\dot{m}_{ice}\left[L_{fus}-Cp_{,ice}T_{equi}\right]+h_c\left(T_{equi}-T_\infty\right)$$

$$+\sigma_o\varepsilon\left[T_{equi}^4-T_\infty{}^4\right]$$

$$h_f\geq 0,\dot{m}_{ice}\geq 0,h_f T_{equi}\geq h_f T_C,\dot{m}_{ice}T_{equi}\leq\dot{m}_{ice}T_C$$

Conjugate (convection-conduction-convection) heat transfer

Poor rotor wake capturing: CFD suffers from excessive numerical dissipation on coarse grids; hence, wake structure and vorticity tend to dissipate rapidly after shedding from rotating blades.

Equations for conductive heat transfer

$$\rho_s C_p(\Delta T)_t=\nabla\cdot\mathbf{Q}-\rho_s(\Delta H/\Delta T),\quad \mathbf{Q}=k_s\nabla(\Delta T)$$

Non-strict hyperbolic equation of droplet movement

The mass loading ratio of the bulk density of the droplets over the bulk density of the air is in the order of 10^{-3} for icing conditions. The weakly coupled algorithm (**one-way coupling**) is applicable.

Lagrangian method

$$\frac{d\mathbf{u}_d}{dt} = C_D \frac{\mathrm{Re}_d}{24K}\left(\mathbf{u}_a - \mathbf{u}_d\right) + \left(1 - \frac{\rho_a}{\rho_w}\right)\frac{1}{Fr^2}\mathbf{g}$$

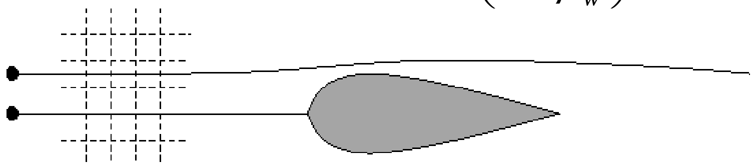

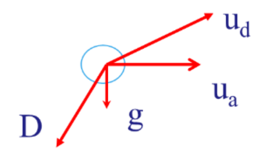

Eulerian method

$$\begin{bmatrix} \rho \\ \rho\mathbf{u} \end{bmatrix}_t + \nabla \cdot \begin{bmatrix} \rho\mathbf{u} \\ \rho\mathbf{uu} \end{bmatrix} = \begin{bmatrix} 0 \\ \mathbf{S}(\rho, \rho_g, T_g, \mathbf{u}, \mathbf{u}_g, \mathbf{g}) \end{bmatrix}$$ Non-strict (degenerate) system

The non-strictly hyperbolic, pressureless gas dynamics type that governs dispersed phase transport within a continuous fluid phase; occurrences of delta shock waves and vacuum states, which bring non-trivial numerical challenges.

Without proper positivity-preserving schemes, the **water droplet density** near the surface, the depth of a dry bed formed by the strong rarefaction wave, may **become negative**.

B. Einfeldt, C. D. Munz, P. L. Roe, B. Sjögreen, "On Godunov-type methods near low densities," *Journal of Computational Physics*, Vol. 92, No. 2, pp. 273-295, 1991.

An idea to overcome the density negativity

$$\begin{bmatrix} \rho \\ \rho \mathbf{u} \end{bmatrix}_t + \nabla \cdot \begin{bmatrix} \rho \mathbf{u} \\ \rho \mathbf{uu} + \rho g d \mathbf{I} \end{bmatrix} = \begin{bmatrix} 0 \\ \mathbf{S}(\rho, \rho_g, T_g, \mathbf{u}, \mathbf{u}_g, \mathbf{g}) \end{bmatrix} + \nabla \cdot \begin{bmatrix} 0 \\ \rho g d \mathbf{I} \end{bmatrix},$$

Well-posed shallow water type Approx. Riemann solver

Simple source treatment

$$\frac{\partial}{\partial t}\int_\Omega \mathbf{U} d\Omega + \oint_{\partial\Omega} \mathbf{H} dl = \int_\Omega \left(\mathbf{S} + \nabla \cdot \begin{bmatrix} 0 \\ \rho g d \mathbf{I} \end{bmatrix} \right) d\Omega$$

$$\frac{\partial \mathbf{U}}{\partial t} = -\frac{1}{\Omega}\left[\oint_{\partial\Omega} \mathbf{H} dl - \int_\Omega (\mathbf{S} + \nabla \cdot \begin{bmatrix} 0 \\ \rho g d \mathbf{I} \end{bmatrix}) d\Omega \right]$$

$$\frac{d\mathbf{U}}{dt} = -\frac{1}{\Omega}\left[\sum_{k=1}^{n} \mathbf{H}_k \Delta l_k - \mathbf{S}\Omega - gd \sum_{k=1}^{n} \rho_k \begin{pmatrix} 0 \\ \mathbf{n}_k \end{pmatrix} \Delta l_k \right]$$

A positivity-preserving upwind scheme based on the characteristic decomposition HLLC approximate Riemann solver

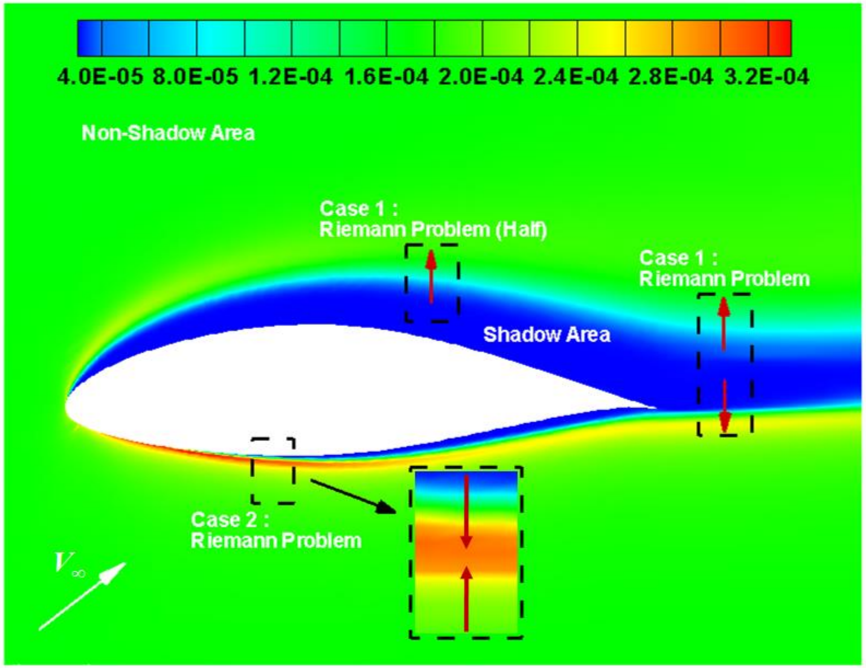

Jung, S. K., Myong, R. S., "A Relaxation Model for Numerical Approximations of the Multidimensional Pressureless Gas Dynamics System," *Computers and Mathematics with Applications*, Vol. 80, No. 5, pp. 1073-1083, 2020.

Importance of rotor wake modeling and hybridization

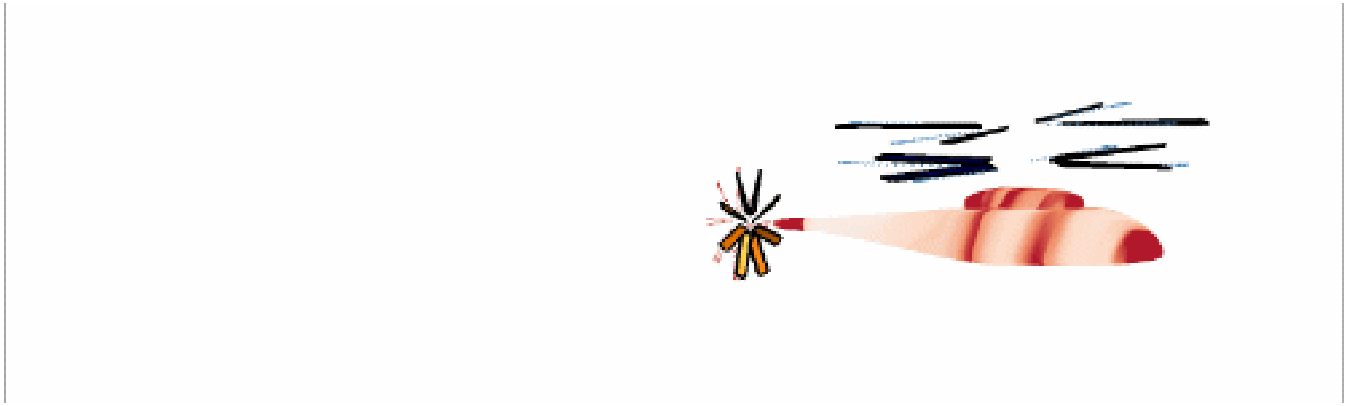

Compound rotorcraft with co-axial rotors
and pusher propellor

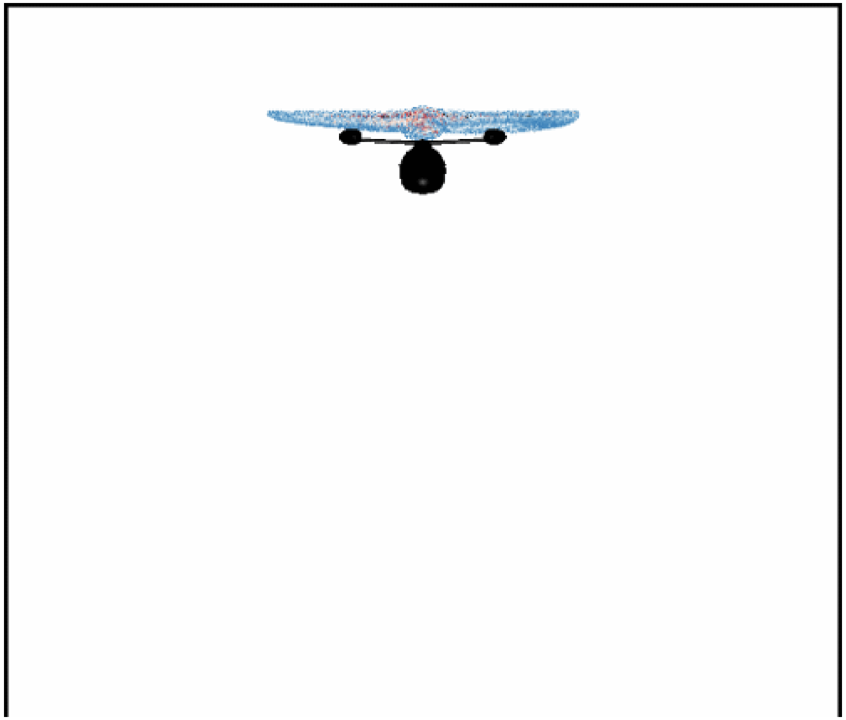

NASA side-by-side urban air mobility

Nonlinear vortex lattice method (NVLM)

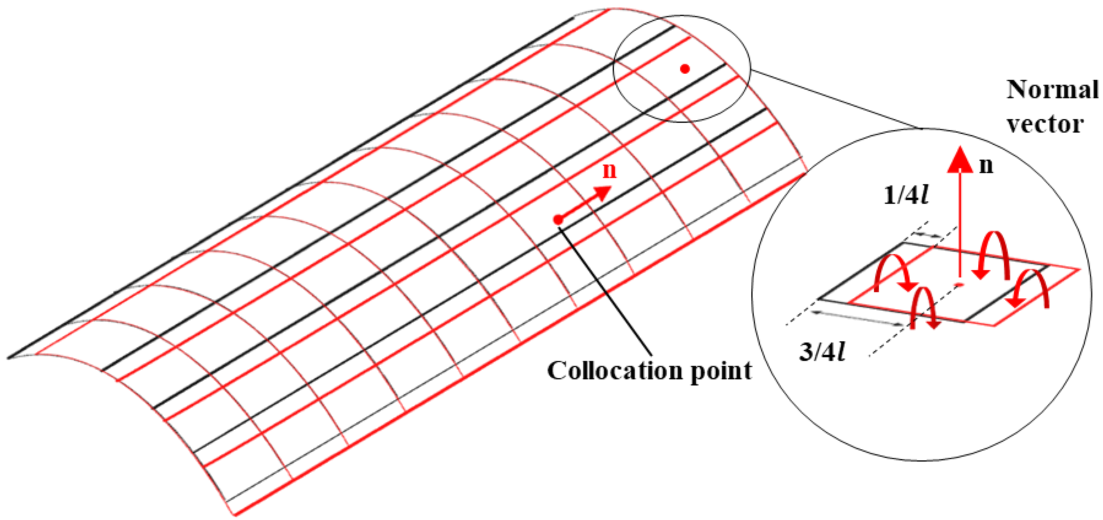

Lee, H., Sengupta, B., Araghizadegh, M. S., Myong, R. S., “Review of Vortex Methods for Rotor Aerodynamics and Wake Dynamics,” *Advances in Aerodynamics*, Vol. 4, 20, 2022.

- Taking nonlinear aerodynamic properties (related to viscosity, flow separation, and low-Reynolds no. flow) into account
- Airfoil look-up tables including stalled flow scenarios
- Semi-empirical models for airfoil aerodynamics in 3-D and rotating settings
- Vortex strength correction to accurately describe the influence of nonlinear aerodynamics on the bound circulation strength

Wake modeling using vortex particle method (VPM)

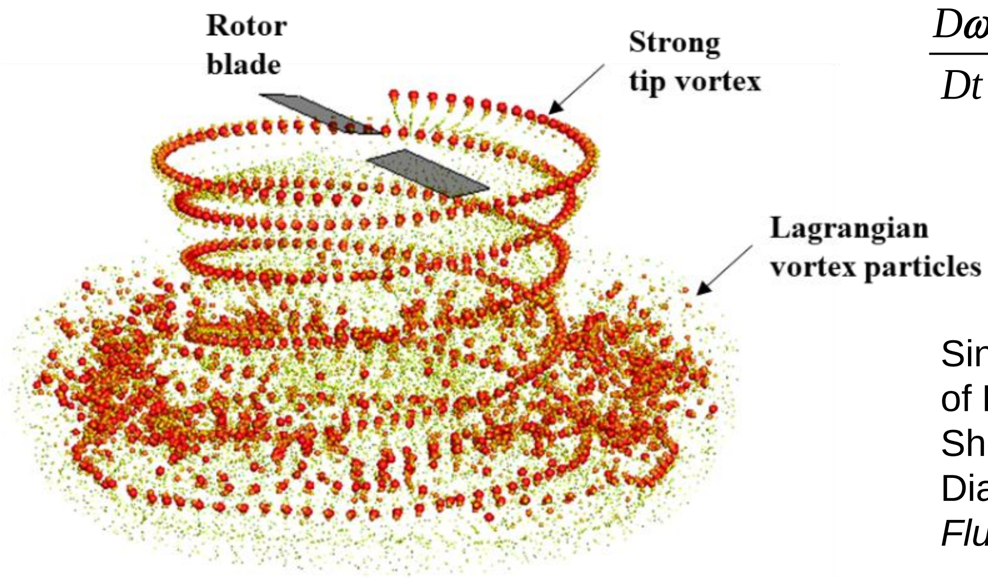

$$\frac{D\boldsymbol{\omega}}{Dt} = (\boldsymbol{\omega}\cdot\nabla)\mathbf{u} - \boldsymbol{\omega}(\nabla\cdot\mathbf{u}) + \frac{1}{\rho^2}\nabla\rho\times\nabla p + \frac{\mu}{\rho}\nabla^2\boldsymbol{\omega} - \frac{\mu}{\rho^2}\nabla\rho\times\nabla^2\mathbf{u} - \frac{\mu}{\rho^2}\nabla\rho\times\nabla(\nabla\cdot\mathbf{u})$$

Singh, S., Battiato, M., Myong, R. S., "Impact of Bulk Viscosity on Flow Morphology of Shock-Accelerated Cylindrical Light Bubble in Diatomic and Polyatomic Gases," *Physics of Fluids*, Vol. 33, 066103, 2021.

- The dominant vortical structures of the rotor wake are the inboard vortex sheet and the tip vortices.
- The geometry of the rotor wake is approximated by a finite number of vortex particles, which are shed from the whole width of the rotor blade.
- The strength of vortex particles is already determined at the previous time step by imposing the Kutta condition at the vortex elements placed on the trailing edges.
- Vortex particles naturally travel downstream with local convection velocity while being permitted to freely distort and interact with one another.

Hybrid method based on NVLM, VPM, and CFD

$$\frac{dx}{dt} = \boldsymbol{u}_{tot} = \boldsymbol{u}_{\infty} + \boldsymbol{u}_{vpm} + \Delta\boldsymbol{u}_{cfd}$$

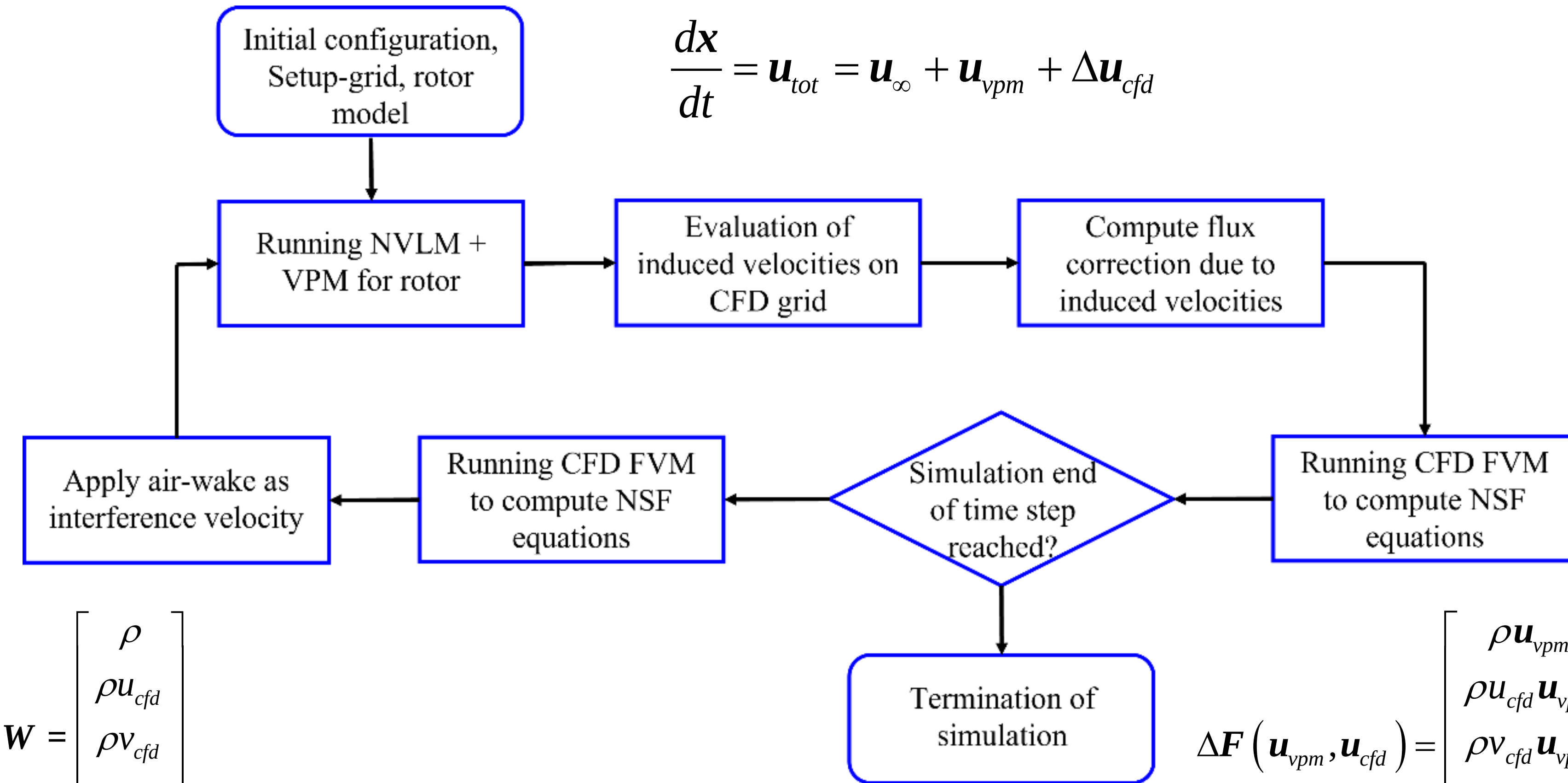

$$\boldsymbol{W} = \begin{bmatrix} \rho \\ \rho u_{cfd} \\ \rho v_{cfd} \\ \rho w_{cfd} \\ \rho E \end{bmatrix}$$

$$\Delta\boldsymbol{F}\left(\boldsymbol{u}_{vpm}, \boldsymbol{u}_{cfd}\right) = \begin{bmatrix} \rho \boldsymbol{u}_{vpm} \cdot \boldsymbol{n} \\ \rho u_{cfd} \boldsymbol{u}_{vpm} \cdot \boldsymbol{n} \\ \rho v_{cfd} \boldsymbol{u}_{vpm} \cdot \boldsymbol{n} \\ \rho w_{cfd} \boldsymbol{u}_{vpm} \cdot \boldsymbol{n} \\ \rho E \boldsymbol{u}_{vpm} \cdot \boldsymbol{n} \end{bmatrix}$$

$$\frac{\partial}{\partial t} \iiint_V \boldsymbol{W}\, dV + \iint_S \left(\boldsymbol{F}_i - \boldsymbol{F}_v + \Delta\boldsymbol{F}\left(\boldsymbol{u}_{vpm}, \boldsymbol{u}_{cfd}\right)\right) \cdot \boldsymbol{n}\, dS = 0$$

Sengupta, B., Prince Raj, L., Esmaeilifar, E., Araghizadeh, M. S., Lee, H., Myong, R. S., "Novel hybrid vortex-CFD approach to rotor wake and ice accretion on rotorcraft," in Review

Novel hybrid vortex-CFD approach

Features	H. Fouladi *et al*. (2013)	C. Son *et al*. (2017)	Present
Rotor modeling	Actuator disk method (ADM) coupled with the momentum equation	Actuator surface method (ASM) coupled with the momentum equation	Non-linear vortex lattice method (NVLM) coupled with the equations of density, momentum, and energy
Rotor wake modeling	Eulerian NSF CFD No explicit modeling	Eulerian NSF CFD No explicit modeling	Lagrangian VPM Explicit modeling
Blade characteristics	Neglects blade geometry	Blade as 2-D surface	Considers 3-D blade geometry (camber, swept angle)
Rotor-wake and wake-fuselage interaction	Does not capture detailed rotor-wake interactions and vortices	Does not explicitly simulate the rotor-wake interactions	Accurately represents rotor-wake and wake-fuselage interactions and vortices with unsteady effects
Airflow solver	Compressible NSF FEM solver	Compressible-PIMPLE segregated NSF FVM solver (OpenFOAM)	Compressible NSF Riemann-based FVM solver (In-house)
Droplet equation	Non-hyperbolic	Non-hyperbolic	Hyperbolic
Unified framework*	No	No	Yes
Computational efficiency	Relatively high computational efficiency	Moderate computational efficiency	Good balance between accuracy and computational efficiency

* Identical discretization methodology (conservative Riemann solver-base FVM) for all the solvers of aerodynamics, droplet impingement, and ice accretion.

Sengupta, B., Prince Raj, L., Esmaeilifar, E., Araghizadeh, M. S., Lee, H., Myong, R. S., “Novel hybrid vortex-CFD approach to rotor wake and ice accretion on rotorcraft,” in Review

Validation: air flow around the ROBIN model

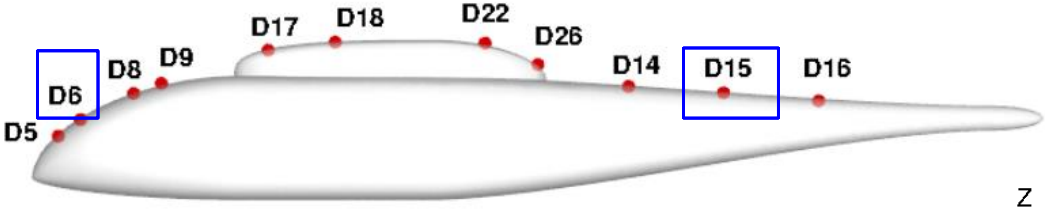

(a) Fuselage Center-line

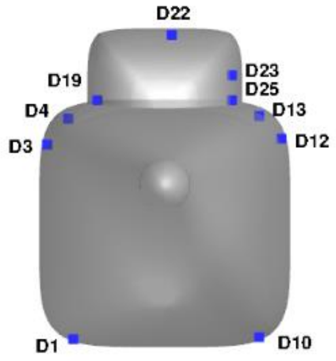

(b) Fuselage Ring, X/L=0.4475

Four-bladed rectangular rotor system
(NACA0012 airfoil with an -8º twist)
Advance ratio of 0.15
Blade tip Mach number of 0.53

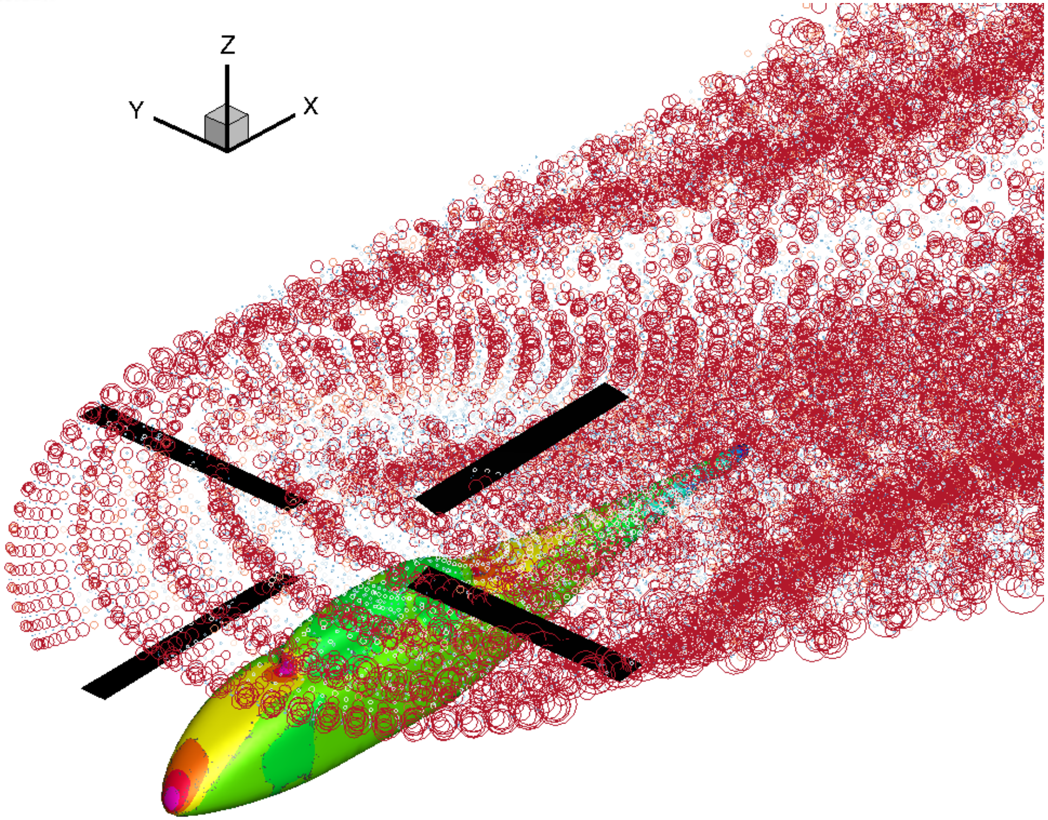

Validation (NVLM+VPM+CFD): *Cp* comparison

Parameter	Value
Target thrust coefficient, C_T [-]	0.0065
Collective pitch angle, θ [deg.]	10.3
Longitudinal cyclic pitch, A1 [deg.]	-2.7
Lateral cyclic pitch, B1 [deg.]	2.4

VLM+VPM+Panel (J. Am. Helicopter Soc. 2014)
VTM (J. Am. Helicopter Soc. 2009)
Euler with an overset mesh (Int. J. Aeronaut. Space Sci. 2010)

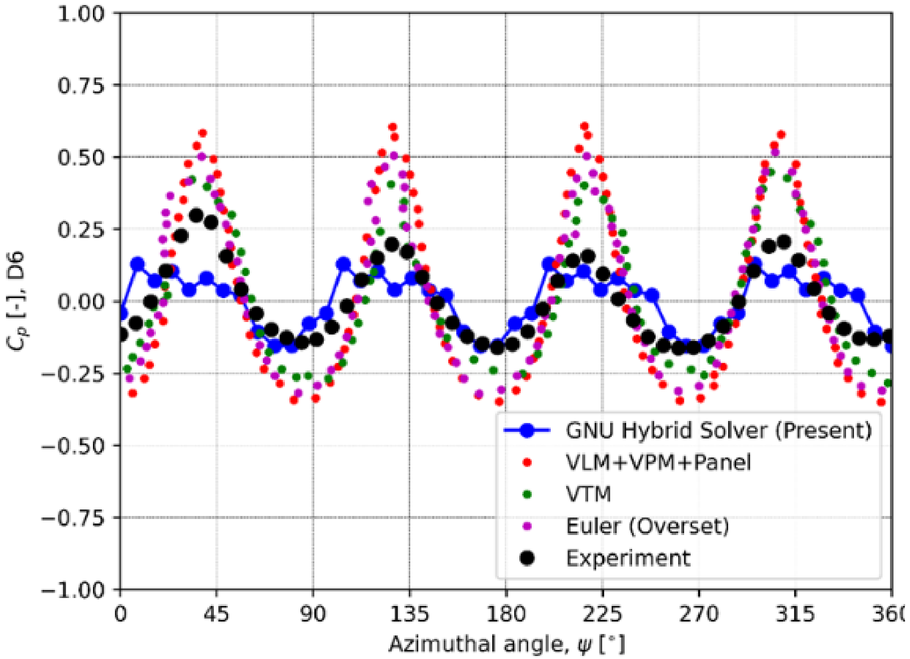

location D6

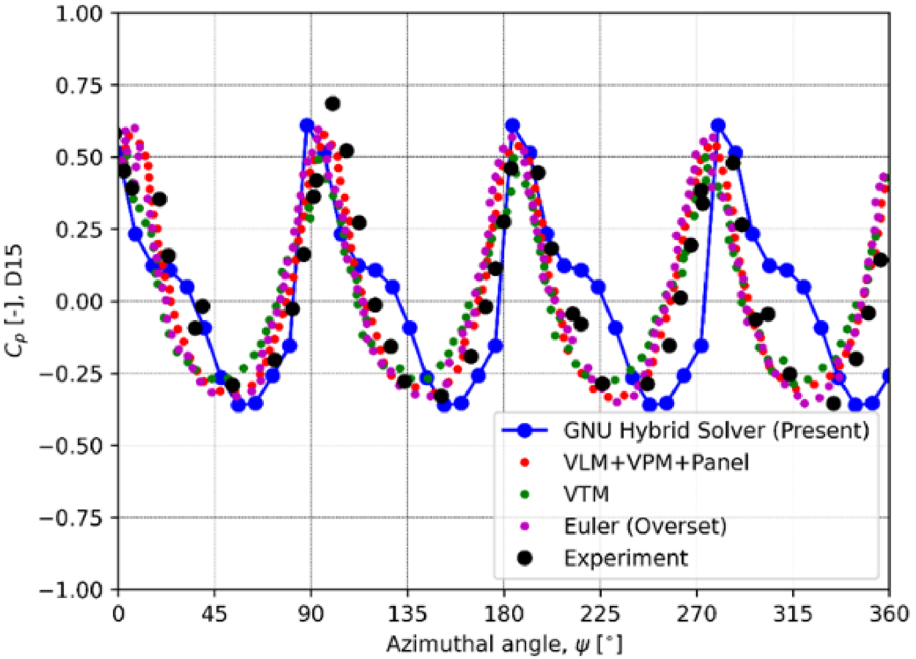

location D15

Coupling of NVLM+VPM+CFD(Air)+CFD(Icing)

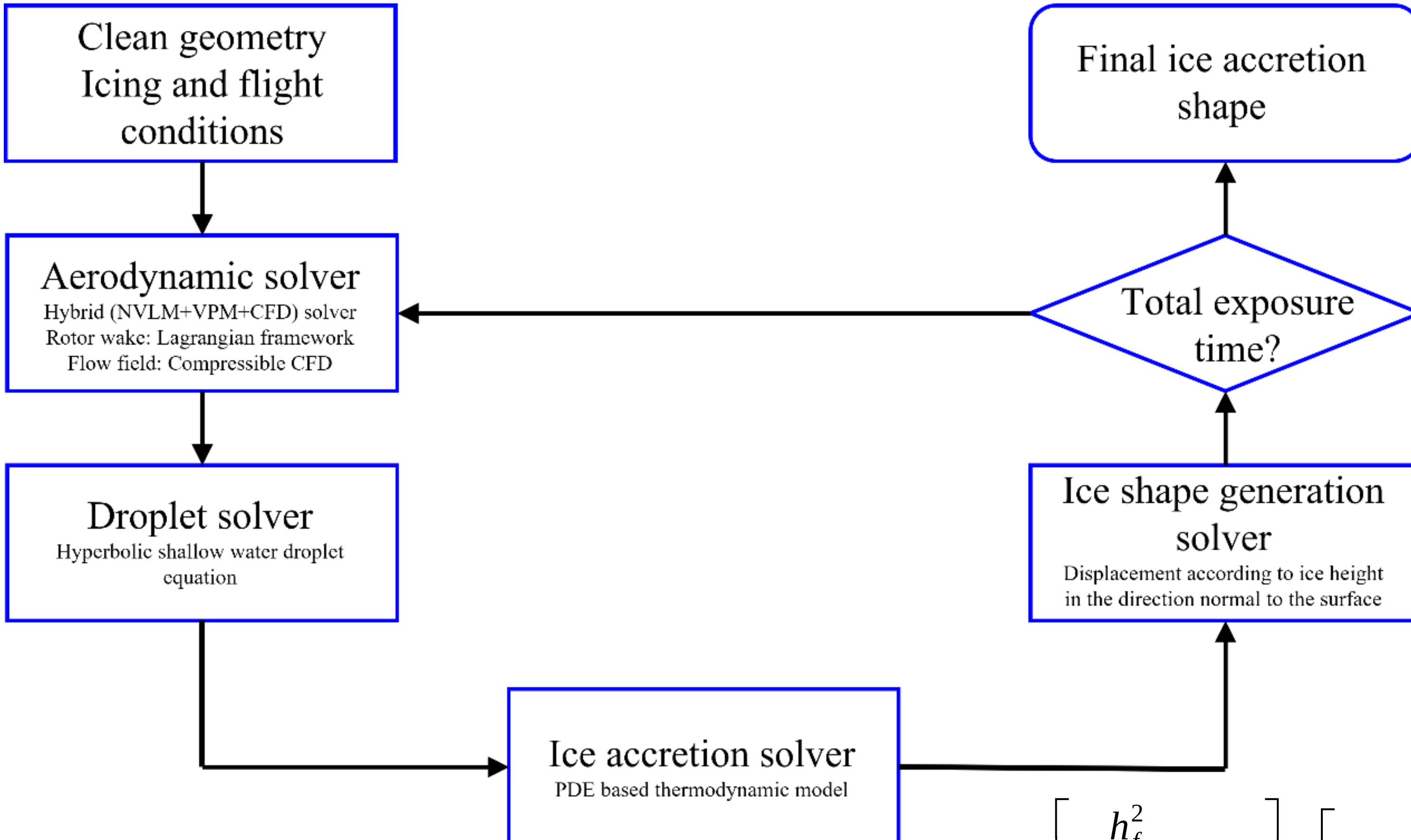

$$\begin{bmatrix}\rho\\ \rho\mathbf{u}\end{bmatrix}_t + \nabla\cdot\begin{bmatrix}\rho\mathbf{u}\\ \rho\mathbf{uu}+\rho g d\mathbf{I}\end{bmatrix} = \begin{bmatrix}0\\ \mathbf{S}_D+\mathbf{S}_G+\mathbf{S}_S\end{bmatrix}$$

$$\begin{bmatrix}h_f\\ h_f T_{equi}\end{bmatrix}_t + \nabla\cdot\begin{bmatrix}\dfrac{h_f^2}{2\mu_w}\tau_{wall}\\ \dfrac{h_f^2 T_{equi}}{2\mu_w}\tau_{wall}\end{bmatrix} = \begin{bmatrix}\dfrac{S_M}{\rho_w}\\ \dfrac{S_E}{\rho_w Cp_{,w}}+\dfrac{T_c S_M}{\rho_w}\end{bmatrix}$$

Visualization of the flow structure (Q-criterion)

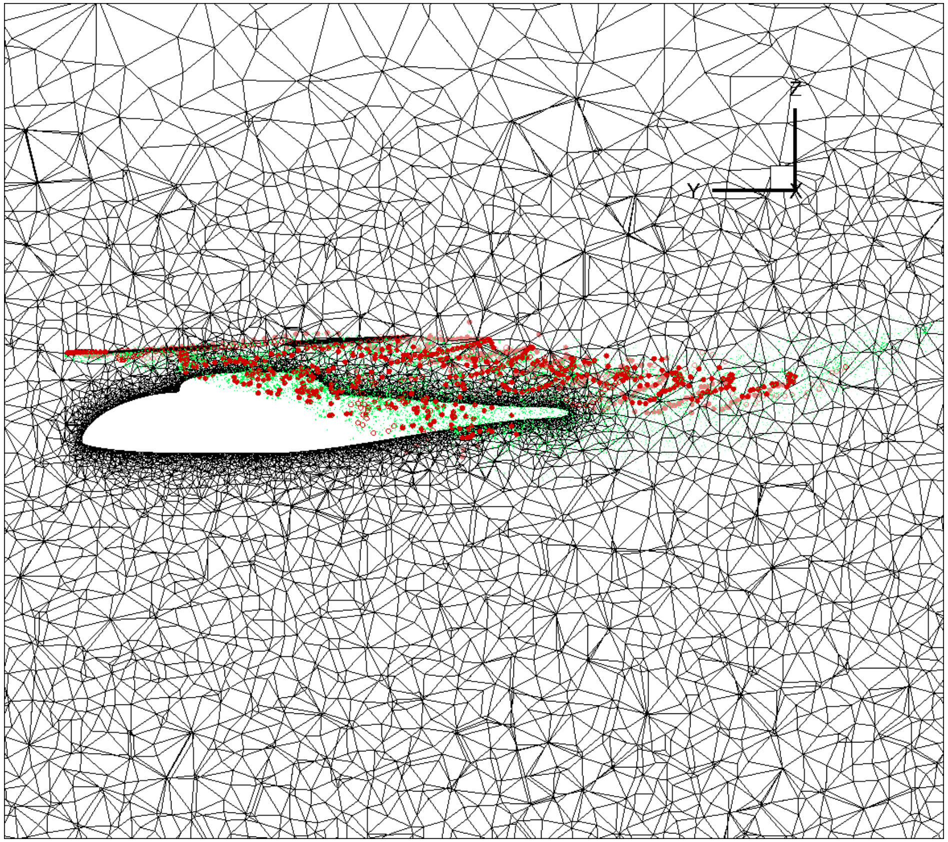

$$Q = \tfrac{1}{2}\left(\Omega_{ij}\Omega_{ij} - S_{ij}S_{ij}\right)$$

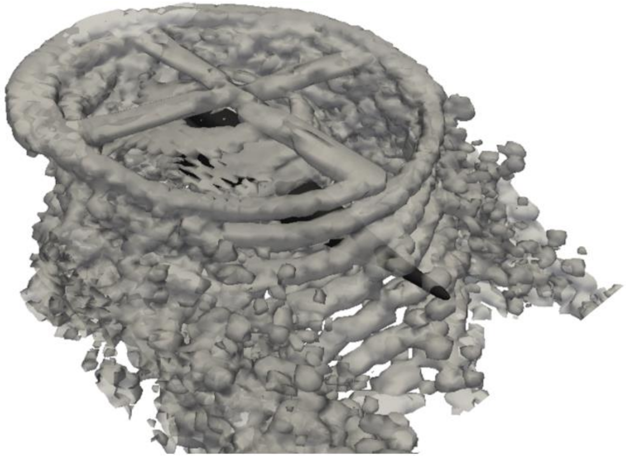

Advance ratio 0.051

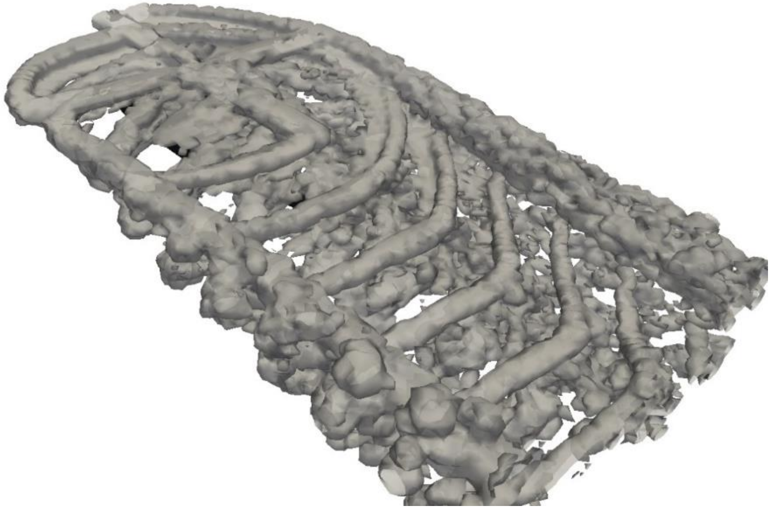

Advance ratio 0.232

Collection efficiency and ice accretion (C_T=0.008)

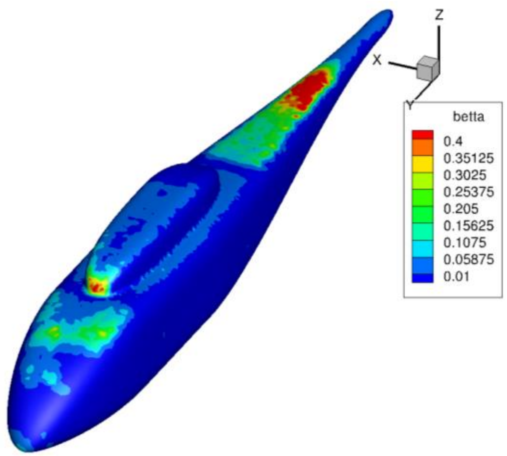

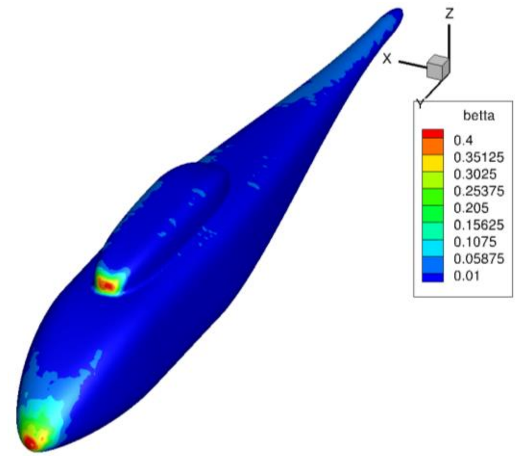

Advance ratio 0.051

Advance ratio 0.232

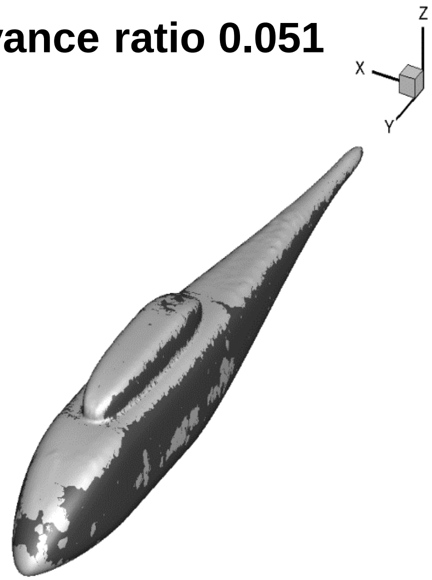

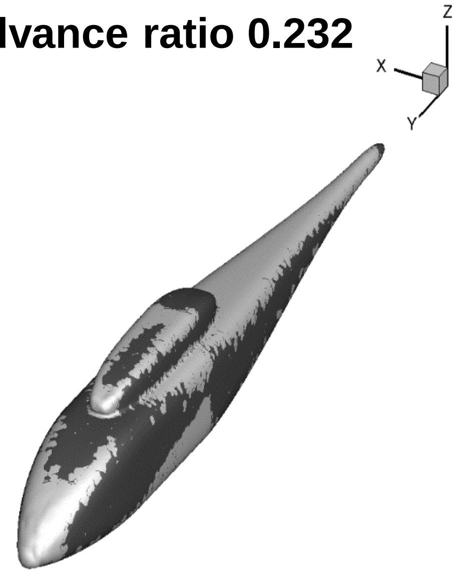

Another critical issue: planetary landings

Planetary landings in outer space is characterized by the **two-phase flow** of compressible gas-particle.

Challenging due to large variations in temperature, particle concentration, including the near-zero limit, and flow velocity, as well as the complexities and nonlinearities of the flow involved in planetary landers with rocket motors.

In a planetary landing, compressible gas-particle flow is formed when the rocket plume of the lander impinges on a dusty surface and causes erosion and dispersal of solid particles into the flow field.

Micro-gravity, vacuum, extreme dryness, unique properties of regolith, multi-scale (m to hundred km) in dispersal

A full continuum Eulerian–Eulerian framework in conjunction with constitutive equations which effectively describes the high non-equilibrium effects in the rarefied condition of the planetary atmosphere based on the second-order nonlinear coupled constitutive relation (NCCR) beyond the conventional first-order NSF constitutive relation.

Lunar landing: Apollo 11

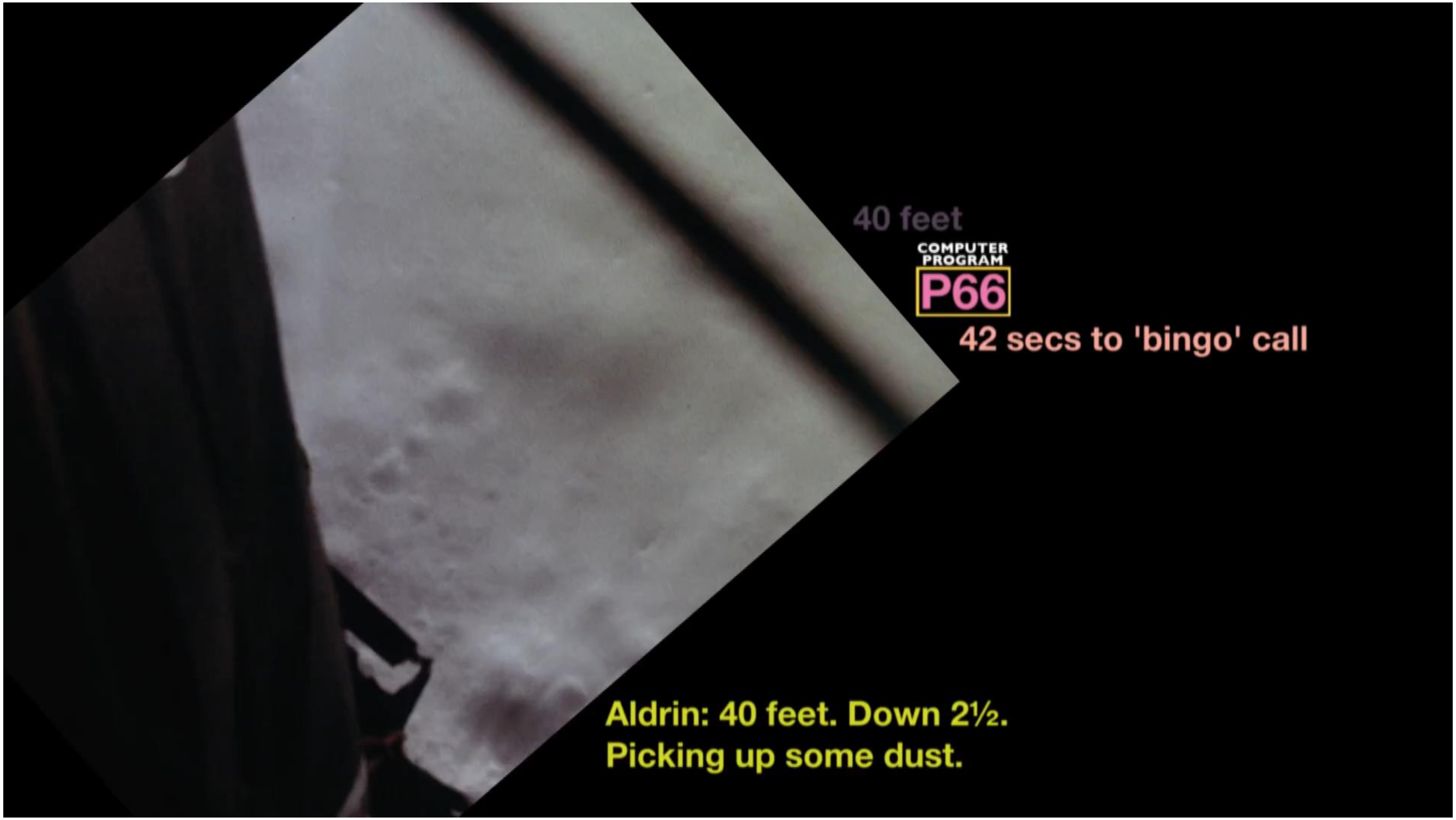

Dust is the number one concern!

Physical damage to lander and sensors

Blocking vision, mal-function of tracking sensor of landing velocity and camera

Trouble in exploration (degradation in thermal-control, dust contamination)

Apollo Astronaut John Young

“Dust is the number one concern in returning to the moon!”

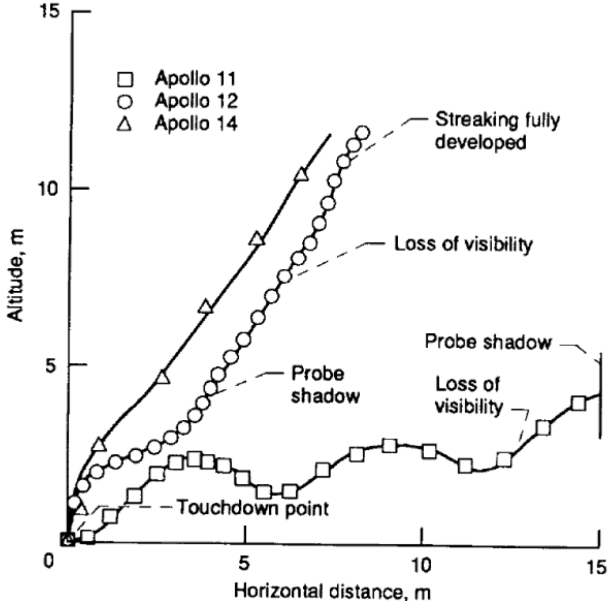

First Lunar landing (Apollo 11)

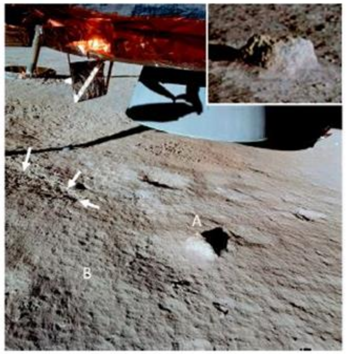

Apollo 14 surface (NASA photograph AS14-66-9261HR)

Lunar surface

Lunar landing problem

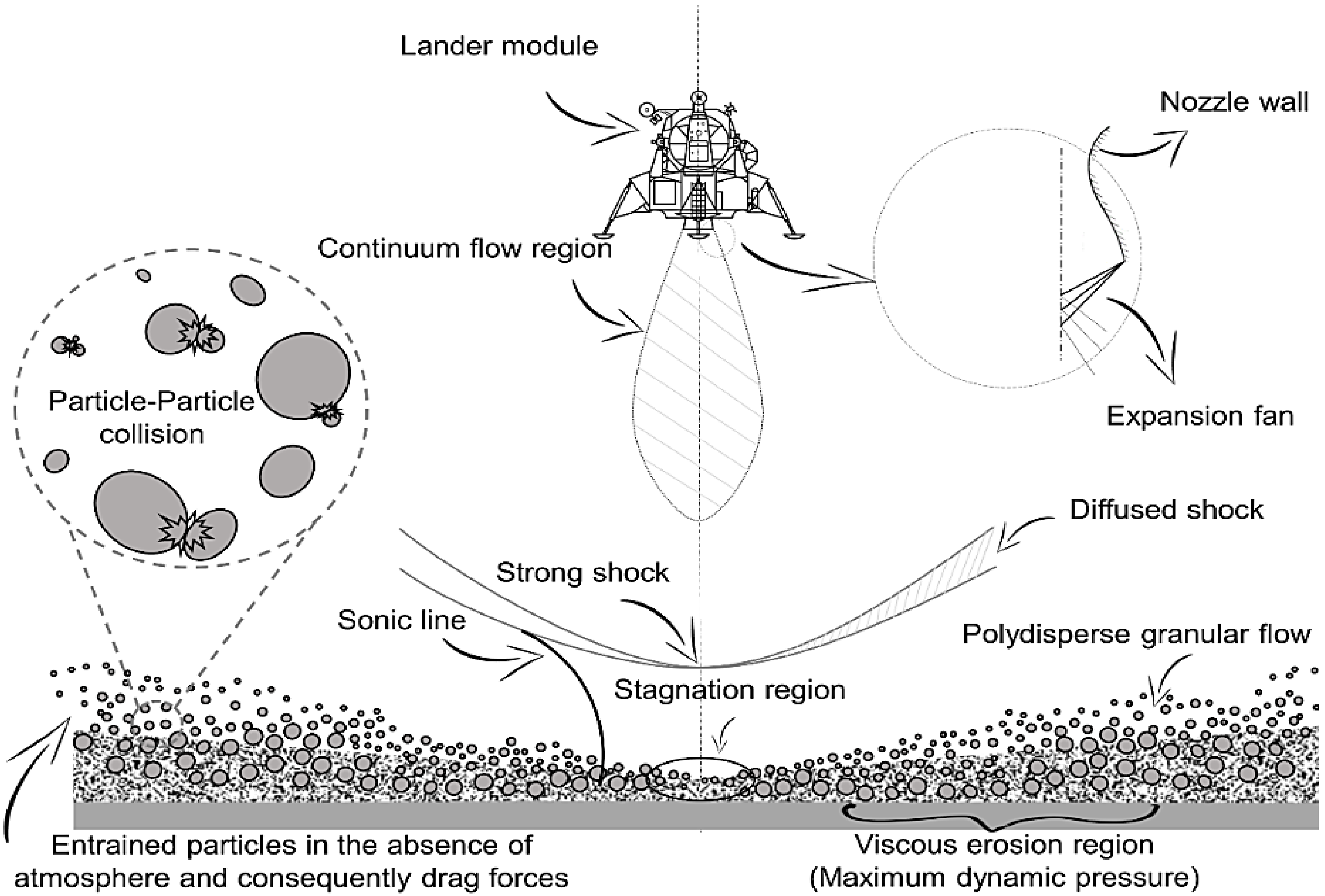

Computational models

Particulate loading

$$\beta = \frac{\alpha_s \rho_s}{\alpha_g \rho_g}$$

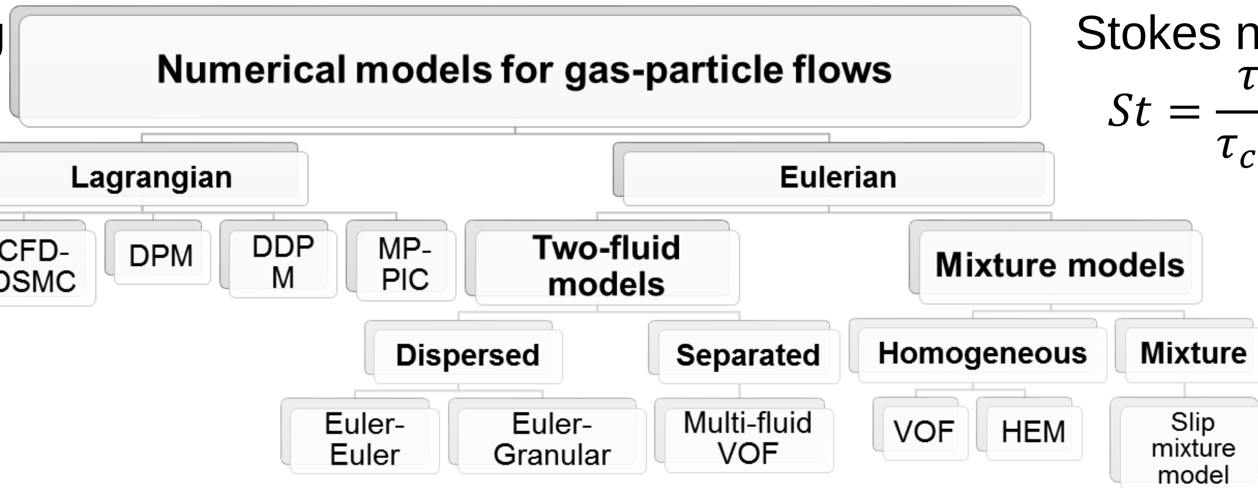

Stokes number

$$St = \frac{\tau_{solid}}{\tau_{carrier}}$$

$$\begin{bmatrix}\alpha_g\rho_g\\ \alpha_g\rho_g\mathbf{u}_g\\ \alpha_g\rho_g E_g\end{bmatrix}_t + \nabla\cdot\begin{bmatrix}\alpha_g\rho_g\mathbf{u}_g\\ \alpha_g\rho_g\mathbf{u}_g\mathbf{u}_g + p_g\mathbf{I}+\mathbf{\Pi}_g\\ (\alpha_g\rho_g E_g+p_g)\mathbf{u}_g+\mathbf{\Pi}_g\cdot\mathbf{u}_g+\mathbf{Q}_g\end{bmatrix} = \nabla\cdot\begin{bmatrix}0\\ D_{g,s}(\mathbf{u}_s-\mathbf{u}_g)\\ D_{g,s}(\mathbf{u}_s-\mathbf{u}_g)\cdot\mathbf{u}_s+Q_{g,s}(T_s-T_g)\end{bmatrix},$$

$$\begin{bmatrix}\alpha_s\rho_s\\ \alpha_s\rho_s\mathbf{u}_s\\ \alpha_s\rho_s E_s\\ \alpha_s\rho_s e_s\end{bmatrix}_t + \nabla\cdot\begin{bmatrix}\alpha_s\rho_s\mathbf{u}_s\\ \alpha_s\rho_s\mathbf{u}_s\mathbf{u}_s + p_s\mathbf{I}+\mathbf{\Pi}_s\\ (\alpha_s\rho_s E_s+p_s)\mathbf{u}_s+\mathbf{\Pi}_s\cdot\mathbf{u}_s+\mathbf{Q}_s\\ \alpha_s\rho_s e_s\mathbf{u}_s\end{bmatrix} = \nabla\cdot\begin{bmatrix}0\\ D_{g,s}(\mathbf{u}_s-\mathbf{u}_g)\\ D_{g,s}(\mathbf{u}_s-\mathbf{u}_g)\cdot\mathbf{u}_s+Q_{g,s}(T_s-T_g)\\ \dot{\gamma}\end{bmatrix},$$

e_s granular temp., $\dot{\gamma}$ the dissipation of pseudo-thermal energy owing to the inelastic particle collisions

Surface erosion model (Roberts' model)

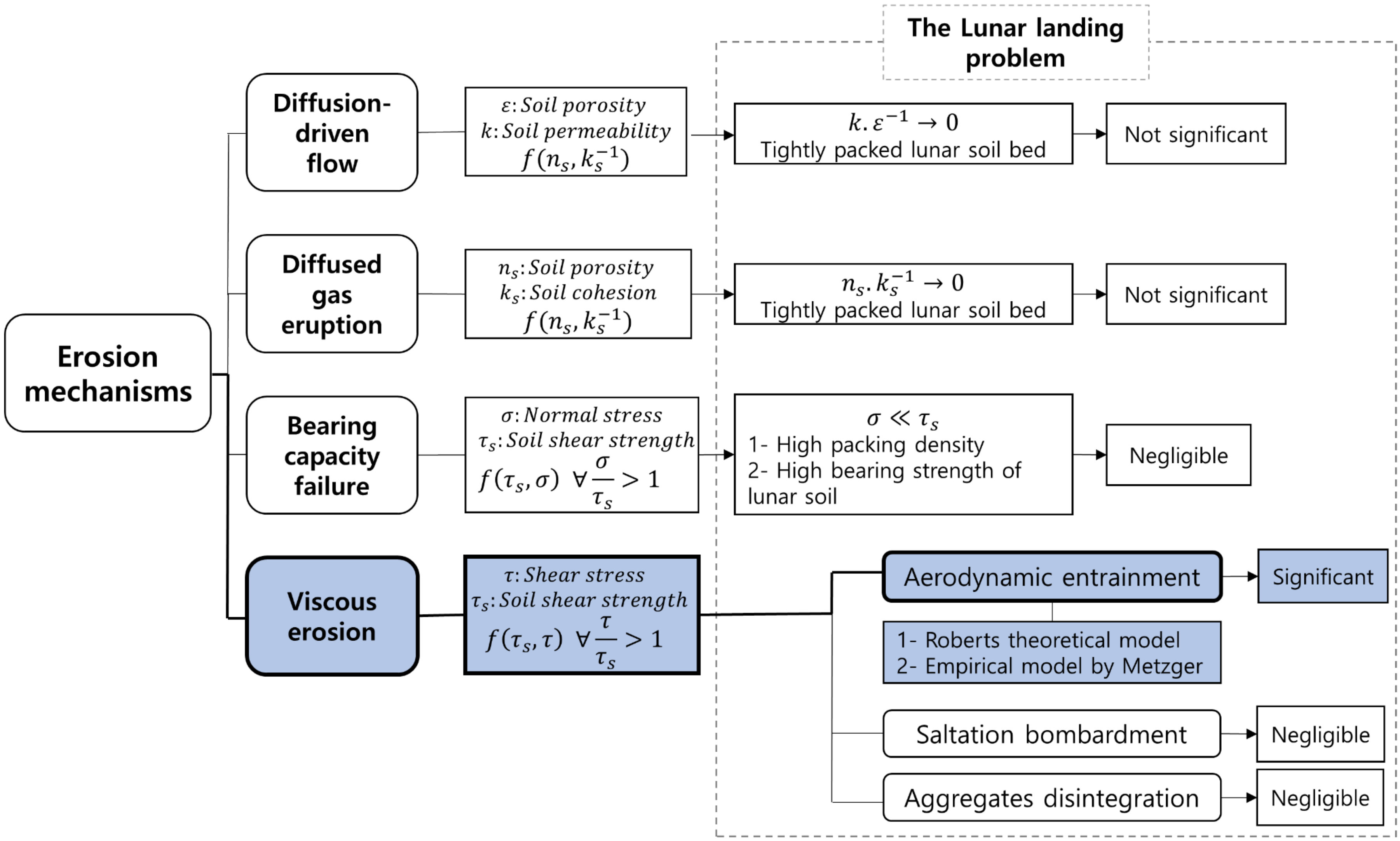

Dispersal simulation from the induced crater

Rahimi, A., Ejtehadi, O., Lee, K. H., Myong, R. S., "Near-field Plume-surface Interaction and Regolith Erosion and Dispersal During the Lunar Landing," *Acta Astronautica*, Vol. 175, pp. 308-326, 2020.

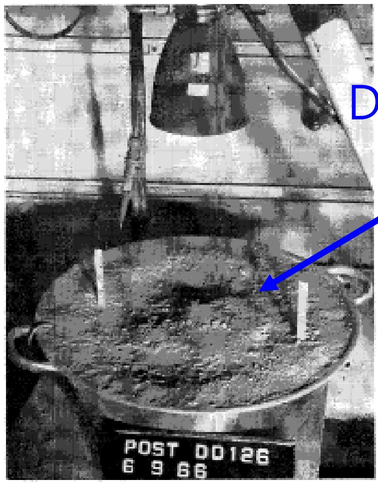

Depth & width

Surface erosion experiment courtesy of Ronald F. Scott 1966

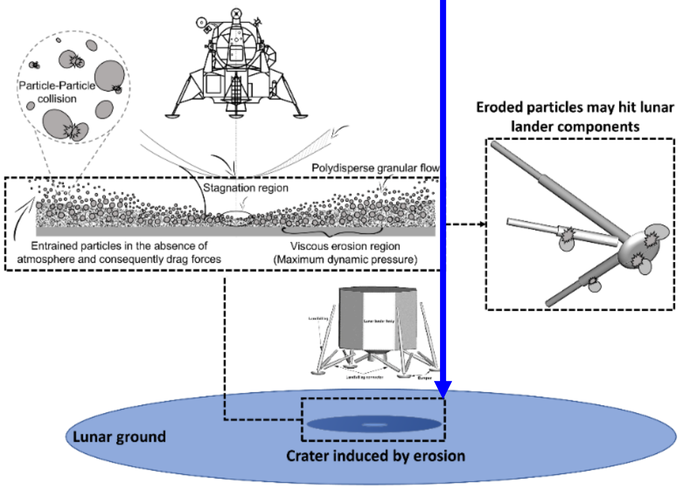

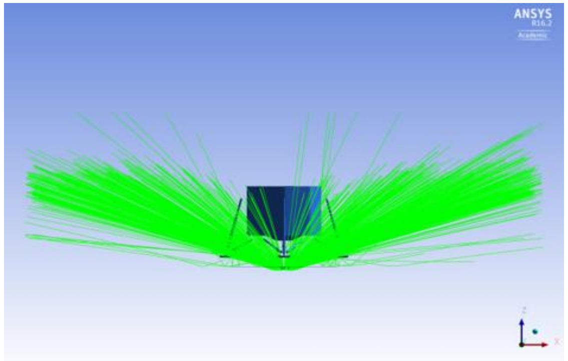

Injected particles with diameter $100\mu m$ and $St = 757$

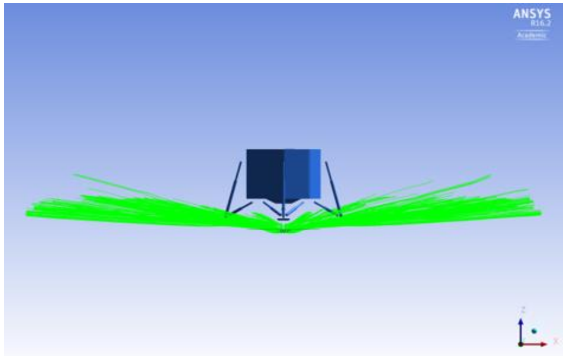

Injected particles with diameter $1\mu m$ and $St = 0.0757$

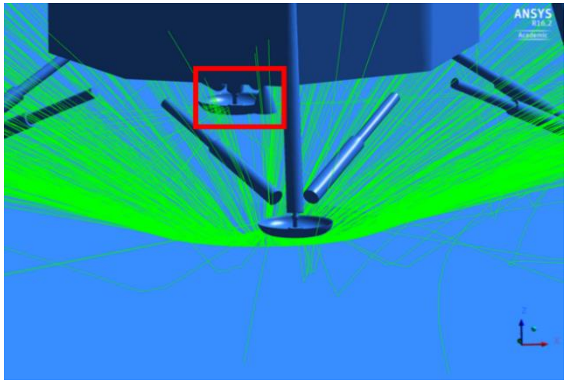

Impingement of particles to the bumper ($100\mu m$)

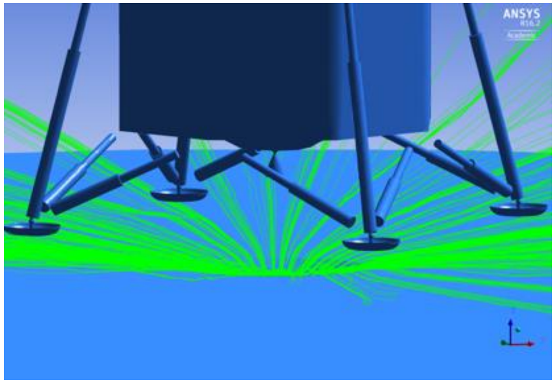

No impingement of particles to the bumper ($1\mu m$)

Classification of gas flows in non-equilibrium

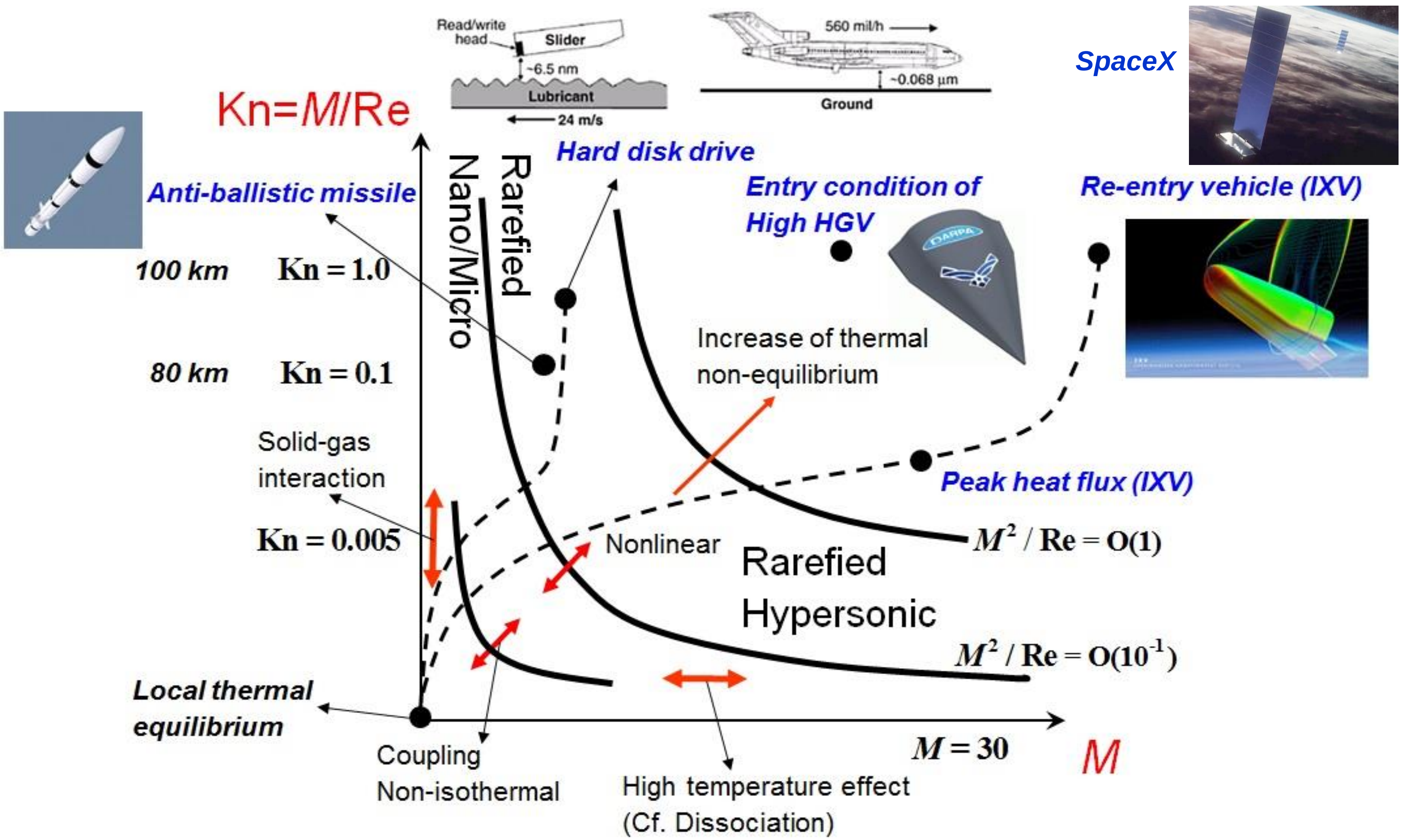

$\mathbf{v}\cdot\nabla f(\mathbf{r},\mathbf{v}) = C[f, f_2]$ $\xrightarrow{\text{M appearing}}$ via statistical average $\rho\mathbf{u}\cdot\nabla\mathbf{u} + \nabla\cdot p\mathbf{I} + \nabla\cdot\mathbf{\Pi} = 0$ $\Longrightarrow$ **Main parameter** $\Pi / p \sim \mathrm{Kn}\cdot M$

Two terms: Kn — **Three terms: *M*, Kn** — **(not Kn alone)** $\dfrac{M^2}{\mathrm{Re}}$ or $\dfrac{M}{\sqrt{\mathrm{Re}}}$

Previous and ongoing studies on NCCR

NCCR: Nonlinear Coupled Constitutive Relation

PoF 1999, JCP 2001, JCP 2004: Eu's generalized hydrodynamics

PoF 2014, PoF 2016: Balanced closure & validation via MD

JCP 2014: 2D hybrid DG code for NCCR

PoF 2018: Polyatomic gases (shock-vortex interaction)

PoF 2020: Topology of NCCR

PoF 2020: Extension to the vibrational mode of energy

JCP 2020: Extension to dusty and granular flows

JCP 2022: 3D hybrid DG code for NCCR

CPC 2023 (Review after Revision): FVM-based *nccrFOAM suite*

Preprint: 2nd-order Boltzmann-type kinetic spring model

Conceptual revision

New closure theory

Physical insight

More validation

Discontinuous Galerkin

Topology

Two-phase flow

Vibrational mode

Viscoelastic flow

Combining with DSMC

Other independent NCCR works: Multi-species extension by Ahn & Kim (SNU, Korea, JCP09)

Implicit-FVM NCCR by Jiang, Zhao, Yuan, Chen (Zhejiang Univ., China, 2017-Present)

Boltzmann kinetic equations

- A first-order partial differential equation of **the probability density of finding a particle in phase space** with an integral collision term

$$\left(\frac{\partial}{\partial t}+\mathbf{v}\cdot\nabla\right)f(t,\mathbf{r},\mathbf{v})=\frac{1}{Kn}C[f,f_2]$$

Movement — Collision (or Interaction)

Kinematic — Dissipation

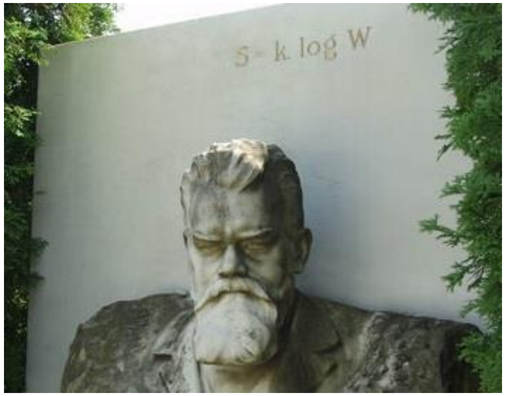

$$C[f,f_2]\sim\int\left|\mathbf{v}-\mathbf{v}_2\right|(f^* f_2^* - ff_2)d\mathbf{v}_2$$

$=$ Gain (scattered into) - Loss (scattered out) = $\left(\frac{\delta f}{\delta t}\right)^+ - \left(\frac{\delta f}{\delta t}\right)^-$

- **Maxwell's equation of transfer** for molecular expression $h^{(n)}$

$$\frac{\partial}{\partial t}\left\langle h^{(n)}f\right\rangle+\nabla\cdot\left(\mathbf{u}\left\langle h^{(n)}f\right\rangle+\left\langle \mathbf{c}h^{(n)}f\right\rangle\right)-\left\langle f\frac{d}{dt}h^{(n)}\right\rangle-\left\langle f\mathbf{c}\cdot\nabla h^{(n)}\right\rangle=\left\langle h^{(n)}C[f,f_2]\right\rangle$$

Moment method and closure theories

$$\phi^{(h)} = \left\langle h^{(k)} f \right\rangle$$

$$\rho\mathbf{u} = \left\langle m\mathbf{v} f(t,\mathbf{r},\mathbf{v}) \right\rangle$$

where

$$\left\langle \cdots \right\rangle = \iiint \cdots dv_x dv_y dv_z$$

$$\phi^{(1)} = \rho,\ \phi^{(2)} = \rho\mathbf{u},\ \phi^{(3)} = \rho E,$$

$$\phi^{(4)} = \mathbf{\Pi} = \left[\mathbf{P}\right]^{(2)},\ \phi^{(5)} = \Delta = \frac{1}{3}\mathrm{Trace}\,\mathbf{P} - p,\ \phi^{(6)} = \mathbf{Q},$$

$$h^{(1)} = m,\ h^{(2)} = m\mathbf{v},\ h^{(3)} = \frac{1}{2}mC^2 + H_{rot},$$

$$h^{(4)} = \left[m\mathbf{CC}\right]^{(2)},\ h^{(5)} = \frac{1}{3}mC^2 - p/n,\ h^{(6)} = \left(\frac{1}{2}mC^2 + H_{rot} - m\hat{h}\right)\mathbf{C},$$

Breakdown of moment method: 1) when the statistical average is meaningless due to too few particles; 2) when thermodynamics is not definable.

Closure-first approach: Grad's 13 moment method (1949) based on **polynomial** expansion

Levermore method (1996) based on **Gaussian** (exponential) expansion

Regularized-13 moment method (2003)

Closure-last balanced approach: Myong's balanced closure (On the High Mach Number Shock Structure Singularity Caused by Overreach of Maxwellian Molecules, PoF 2014)

Relationship with conservation laws (moments)

Boltzmann transport equation (BTE): 10^{23}

$$\left(\frac{\partial}{\partial t}+\mathbf{v}\cdot\nabla\right)f(t,\mathbf{r},\mathbf{v})=C[f,f_2]$$

$$\rho\mathbf{u}=\langle m\mathbf{v}f(t,\mathbf{r},\mathbf{v})\rangle$$

where $\langle\cdots\rangle=\iiint\cdots dv_x dv_y dv_z$

Differentiating the statistical definition $\rho\mathbf{u}\equiv\langle m\mathbf{v}f(t,\mathbf{r},\mathbf{v})\rangle$ *with time* and *then combining* with BKE ($t,\mathbf{r},\mathbf{v}$ are independent and $\mathbf{v}=\mathbf{u}+\mathbf{c}$)

$$\frac{\partial}{\partial t}\langle m\mathbf{v}f\rangle=\left\langle m\mathbf{v}\frac{\partial f}{\partial t}\right\rangle=-\langle m(\mathbf{v}\cdot\nabla f)\mathbf{v}\rangle+\langle m\mathbf{v}C[f,f_2]\rangle$$

$[\mathbf{A}]^{(2)}$: Traceless symmetric part of tensor $\mathbf{A}$

Here $-\langle m(\mathbf{v}\cdot\nabla f)\mathbf{v}\rangle=-\nabla\cdot\langle m\mathbf{v}\mathbf{v}f\rangle=-\nabla\cdot\{\rho\mathbf{u}\mathbf{u}+\langle m\mathbf{c}\mathbf{c}f\rangle\}$

After the decomposition of the stress into pressure and viscous shear stress

$\mathbf{P}\equiv\langle m\mathbf{c}\mathbf{c}f\rangle=p\mathbf{I}+\mathbf{\Pi}$ where $p\equiv\langle m\mathrm{Tr}(\mathbf{c}\mathbf{c})f/3\rangle$, $\mathbf{\Pi}\equiv\langle m[\mathbf{c}\mathbf{c}]^{(2)}f\rangle$,

and using the collisional invariance of the momentum, $\langle m\mathbf{v}C[f,f_2]\rangle=0$, we have

$$\frac{\partial(\rho\mathbf{u})}{\partial t}+\nabla\cdot(\rho\mathbf{u}\mathbf{u}+p\mathbf{I}+\mathbf{\Pi})=0$$

Conservation laws: 13

Closing-last balanced closure on open terms

$$\mathbf{\Pi} \equiv \left\langle m[\mathbf{cc}]^{(2)} f \right\rangle$$

Closure theory: how, where (open terms), when (last)

New balanced closure with closure-last approach (PoF 2014)

2nd-order for kinematic LH = 2nd-order for collsion RH

$$\frac{D}{Dt}(\mathbf{\Pi}/\rho) + \boxed{\nabla \cdot \Psi^{(\Pi)}} + 2[\mathbf{\Pi} \cdot \nabla \mathbf{u}]^{(2)} + 2p[\nabla \mathbf{u}]^{(2)} = \boxed{\left\langle m[\mathbf{cc}]^{(2)} C[f, f_2] \right\rangle \left(\equiv \mathbf{\Lambda}^{(\Pi)}\right)}$$

2nd-order closure

2nd-order closure

$$\underset{2nd}{=} -\frac{p}{\mu_{NS}} \mathbf{\Pi} q_{2nd}(\kappa_1) \text{ where } \Psi^{(\Pi)} = \langle m\mathbf{ccc}f \rangle - \langle m\mathrm{Tr}(\mathbf{ccc}) f \rangle \mathbf{I}/3$$

$$\frac{D}{Dt}\left(\Psi^{(\Pi)}/\rho\right) + \nabla \cdot \Xi + \cdots = \left\langle h^{(\Psi^{(\Pi)})} C[f, f_2] \right\rangle$$

Closure of dissipation terms via 2nd-law

Key ideas; exponential canonical form, consideration of entropy production σ, and non-polynomial expansion called as cumulant expansion (B. C. Eu in 80-90s)

By writing the distribution function f in the exponential form

$$f = \exp\left[-\beta\left(\frac{1}{2}mc^2 + \sum_{n=1}^{\boxed{\infty}} X^{(n)}h^{(n)} - N\right)\right],\ \beta \equiv \frac{1}{k_B T},$$

Nonequilibrium entropy Ψ: $\Psi(\mathbf{r},t) = -k_B\left\langle\left[\ln f(\mathbf{v},\mathbf{r},t) - 1\right] f(\mathbf{v},\mathbf{r},t)\right\rangle,$

Nonequilibrium entropy production: $\sigma_c \equiv -k_B\left\langle \ln f\ \ C[f, f_2]\right\rangle$

When f is truncated, it is truncated in such as way that the divergence problem related to the heat flux contribution containing the 3rd order term for the integrand would not arise (Al-Ghoul, M., and Eu, B. C., Nonequilibrium Partition Function in the Presence of Heat Flow, J. Chem. Phys., Vol. 115, No. 18, 2001).

$$\sigma_c = \frac{1}{4}k_B\int d\mathbf{v}\int d\mathbf{v}_2\int_0^{2\pi} d\phi\int_0^{\infty} db\ bg_{12}\ln(f^{c*}f_2^{c*}/f^c f_2^c)(f^{c*}f_2^{c*} - f^c f_2^c) \geq 0 \ (\text{satisfying 2nd-law})$$

$$\sigma_c \equiv -k_B\left\langle \ln f\ \ C[f, f_2]\right\rangle = \frac{1}{T}\left\langle\left(\frac{1}{2}mc^2 + \sum_{n=1}^{\infty} X^{(n)} : h^{(n)} - N\right) C[f^{(0)}\exp(-x), f_2^{(0)}\exp(-x_2)\right\rangle$$

$$= \frac{1}{4}k_B\int d\mathbf{v}\int d\mathbf{v}_2\int_0^{2\pi} d\phi\int_0^{\infty} db\ bg_{12} f^{(0)} f_2^{(0)}(x_{12} - y_{12})\left[\exp(-y_{12}) - \exp(-x_{12})\right]$$

$$= \frac{1}{4T}\int d\Gamma_{12} f^{(0)} f_2^{(0)}(x_{12} - y_{12})\left[\exp(-y_{12}) - \exp(-x_{12})\right], \quad \left(\begin{array}{l} x \equiv \beta\left(\sum_{n=1}^{\infty} X^{(n)}h^{(n)} - N\right), \\ y \text{ the post-collision value of } x \end{array}\right)$$

$$\sigma_c = \kappa_1^2 q(\kappa_1^{(\pm)}, \kappa_2^{(\pm)}, \cdots) \text{ via cumulant expansion } \left(\kappa_1 \equiv \frac{1}{2}\left\{\left\langle\left(x_{12} - y_{12}\right)^2\right\rangle_c\right\}^{1/2}\right)$$

$$\text{where } q(\kappa_1^{(\pm)}, \kappa_2^{(\pm)}, \cdots) \equiv \frac{1}{2\kappa_1}\left\{\exp\left[\sum_{l=1}^{\infty}\frac{(-1)^l}{l!}\kappa_l^{(+)}\right] - \exp\left[\sum_{l=1}^{\infty}\frac{(-1)^l}{l!}\kappa_l^{(-)}\right]\right\}$$

Cumulant expansion method

$$\langle x^l \rangle = \int x^l f(x)dx,\ \ \langle e^{\lambda x}\rangle = \int e^{\lambda x} f(x)dx$$

Then we have

$$\langle e^{\lambda x}\rangle = \sum_{l=0}^{\infty} \frac{\lambda^l}{l!}\langle x^l\rangle = \boxed{\exp\left[\sum_{l=1}^{\infty} \frac{\lambda^l}{l!}\kappa_l\right]} \text{ where}$$

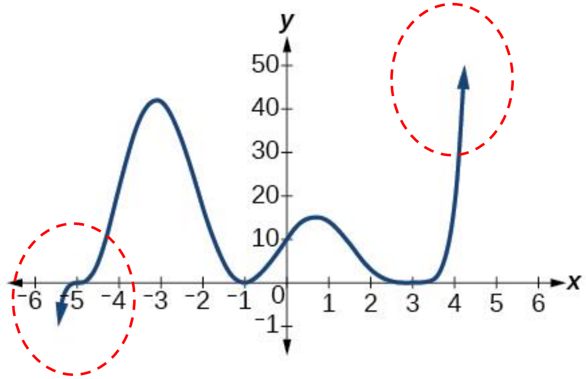

$$\kappa_l = \left[\frac{d^l}{d\lambda^l}\ln\langle e^{\lambda x}\rangle\right]_{\lambda=0};\ \kappa_1 = \langle x\rangle,\ \kappa_2 = \langle x^2\rangle - \langle x\rangle^2, \cdots \text{ (mean, variance)}$$

$$\langle e^x\rangle_{\text{polynomical}} = 1 + \langle x\rangle + \frac{1}{2!}\langle x^2\rangle + \frac{1}{3!}\langle x^3\rangle + \cdots,$$

$$\langle e^x\rangle_{\text{cumulant}} = \exp^{\left[\langle x\rangle + \frac{1}{2!}\left(\langle x^2\rangle - \langle x\rangle^2\right) + \cdots\right]}$$

$$\left(\langle e^x\rangle - \langle e^{-x}\rangle\right)/2\Big]_{\text{polynomial}} = \langle x\rangle + \frac{1}{3}\langle x^3\rangle + \cdots \approx \langle x\rangle$$

$$\left(\langle e^x\rangle - \langle e^{-x}\rangle\right)/2\Big]_{\text{cumulant}} = \exp^{\left(\frac{1}{2!}\left(\langle x^2\rangle - \langle x\rangle^2\right) + \cdots\right)}\left[\exp^{(\langle x\rangle + \cdots)} - \exp^{(-\langle x\rangle + \cdots)}\right]/2 \underset{2nd}{\approx} \sinh\langle x\rangle$$

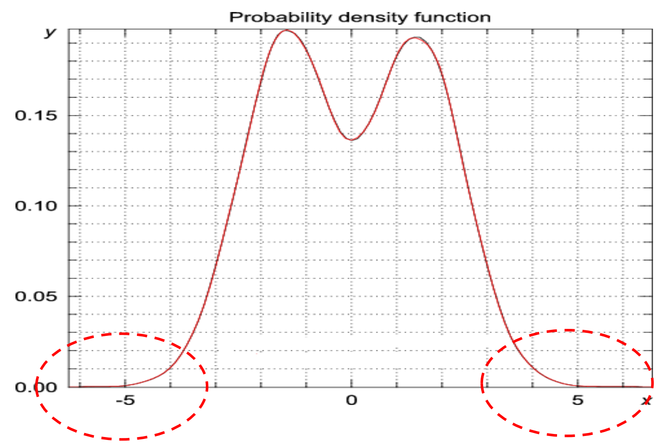

R. S. Myong, Gyeongsang National University, Republic of Korea

Closure of dissipation terms-continued

$$\sigma_c \equiv -k_B \langle \ln f \; C[f, f_2] \rangle = \frac{1}{T}\sum_{n=1}^{\infty} X^{(n)} \langle h^{(n)} C[f, f_2] \rangle = \frac{1}{T}\sum_{l=1}^{\infty} X^{(n)} \Lambda^{(n)} = \kappa_1^2 q(\kappa_1^{(\pm)}, \kappa_2^{(\pm)}, \cdots) \,,$$

Calculating the first reduced collision integral κ_1 in terms of $X^{(n)}$,

$\kappa_1^2 = \sum_{n,l=1}^{\infty} X^{(n)} R_{12}^{(nl)} X_2^{(l)}$, where $R_{12}^{(nl)}$ are coefficients made up of collision bracket integrals,

$$\mathbf{\Lambda}^{(n)} = \frac{1}{\beta g}\sum_{l=1}^{\infty} R_{12}^{(nl)} X_2^{(l)} q(\kappa_1^{(\pm)}, \kappa_2^{(\pm)}, \cdots)$$

After generalizing the equilibrium Gibbs ensemble theory to nonequilibrium processes,

one can obtain the leading order terms for $X^{(n)}$, $X^{(1)} = -\dfrac{\mathbf{\Pi}}{2p}$, $X^{(2)} = -\dfrac{\mathbf{Q}}{pC_pT}$.

Finally, a thermodynamically-consistent constitutive equation, still exact to BKE, can be derived;

$$\rho\frac{D(\mathbf{\Pi}/\rho)}{Dt} + \boxed{\nabla\cdot\mathbf{\Psi}^{(\Pi)}} + 2[\mathbf{\Pi}\cdot\nabla\mathbf{u}]^{(2)} + 2p[\nabla\mathbf{u}]^{(2)} = \boxed{\frac{1}{\beta g}\sum_{l=1}^{\infty} R_{12}^{(2l)} X_2^{(l)} q(\kappa_1^{(\pm)}, \kappa_2^{(\pm)}, \cdots)}$$

$$\rho\frac{D(\mathbf{Q}/\rho)}{Dt} + \boxed{\nabla\cdot\mathbf{\Psi}^{(Q)} + \mathbf{\Psi}^{(P)}\cdot\nabla\mathbf{u}} + \frac{D\mathbf{u}}{Dt}\cdot\mathbf{\Pi} + \mathbf{Q}\cdot\nabla\mathbf{u} + \mathbf{\Pi}\cdot C_p\nabla T + pC_p\nabla T$$

$$= \boxed{\frac{1}{\beta g}\sum_{l=1}^{\infty} R_{12}^{(3l)} X_2^{(l)} q(\kappa_1^{(\pm)}, \kappa_2^{(\pm)}, \cdots)}$$

2^{nd}-order NCCR model

Conservation laws (exact consequence of BKE)

$$\frac{\partial(\rho\mathbf{u})}{\partial t}+\nabla\cdot\left(\rho\mathbf{u}\mathbf{u}+p\mathbf{I}+\mathbf{\Pi}\right)=\mathbf{0}$$

in conjunction with the 2^{nd}-order constitutive relations (CR)

Zero in 2^{nd}-order approximation

$$\frac{\partial\mathbf{\Pi}}{\partial t}+\mathbf{u}\cdot\nabla\mathbf{\Pi}+\cancel{\nabla\cdot\Psi^{(\Pi)}}+2\left[\mathbf{\Pi}\cdot\nabla\mathbf{u}\right]^{(2)}+2p\left[\nabla\mathbf{u}\right]^{(2)}=-\frac{p}{\mu_{NS}}\mathbf{\Pi}q_{2nd}(\kappa_1),$$

Non-local term **2^{nd}-order coupling** **Navier 1^{st} law**

$$\Psi^{(\Pi)}\equiv\left\langle m\mathbf{ccc}f\right\rangle-\left\langle m\mathrm{Tr}(\mathbf{ccc})f\right\rangle\mathbf{I}/3$$

$$q_{2nd}(\kappa_1)\equiv\frac{\sinh\kappa_1}{\kappa_1},\quad \kappa_1\equiv\frac{T^{1/4}}{p}\left(\frac{\mathbf{\Pi}:\mathbf{\Pi}}{\mu_{NS}}+\frac{\mathbf{Q}\cdot\mathbf{Q}/T}{k_{NS}}\right)^{1/2}$$

Onsager-Rayleigh dissipation function

Sinh{1^{st}-order theory}

Navier-Fourier laws inclusive like onion!

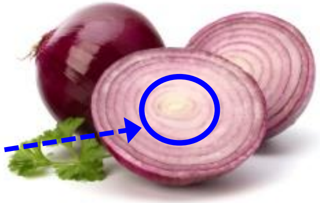

3D mixed modal DG method for the 2nd-order model

$$\partial_t \mathbf{U} + \nabla \mathbf{F}_{\text{inv}}(\mathbf{U}) + \nabla \mathbf{F}_{\text{vis}}(\mathbf{U}, \nabla \mathbf{U}) = 0$$

Singh, S., Karchani, A., Chourushi, T., Myong, R. S., A Three-Dimensional Modal Discontinuous Galerkin Method for the Second-Order Boltzmann-Curtiss-Based Constitutive Model of Rarefied and Microscale Gas Flows, *Journal of Computational Physics*, Vol. 457, 111052, 2022

Discretization in mixed form

$$\begin{cases} \boxed{\mathbf{S} - \nabla \mathbf{U} = 0} \\ \partial_t \mathbf{U} + \nabla \mathbf{F}_{\text{inv}}(\mathbf{U}) + \nabla \mathbf{F}_{\text{vis}}(\mathbf{U}, \mathbf{S}) = 0 \end{cases}$$

NSF model $(\mathbf{\Pi}, \mathbf{Q}) = \mathbf{f}_{\text{linear}}(\mathbf{S}(\mathbf{U}))$

$\boxed{\text{NCCR model } (\mathbf{\Pi}, \mathbf{Q})_{\text{NCCR}} = \mathbf{f}_{\text{non-linear}}(\mathbf{S}(\mathbf{U}), p, T)}$

NCCR: Nonlinear Coupled Constitutive Relation

$$\mathbf{U}_h(\mathbf{x}, t) = \sum_{i=0}^{k} U_j^i(t)\varphi^i(\mathbf{x}), \quad \mathbf{S}_h(\mathbf{x}, t) = \sum_{i=0}^{k} S_j^i(t)\varphi^i(\mathbf{x})$$

$$\begin{cases} \dfrac{\partial}{\partial t}\displaystyle\int_I \mathbf{U}\varphi dV - \int_I \nabla\varphi \mathbf{F}_{\text{inv}} dV + \int_{\partial I} \varphi \mathbf{F}_{\text{inv}} \cdot \mathbf{n} d\Gamma - \int_I \nabla\varphi \mathbf{F}_{\text{vis}} dV + \int_{\partial I} \varphi \mathbf{F}_{\text{vis}} \cdot \mathbf{n} d\Gamma = 0, \\ \displaystyle\int_I \mathbf{S}\varphi dV + \int_I T^s \nabla\varphi \mathbf{U} dV - \int_{\partial I} T^s \varphi \mathbf{U} \cdot \mathbf{n} d\Gamma = 0, \end{cases}$$

Dubiner basis function, Lax-Friedrichs inviscid flux, central flux for viscous terms

Decomposition of NCCR for multi-dimensional flow

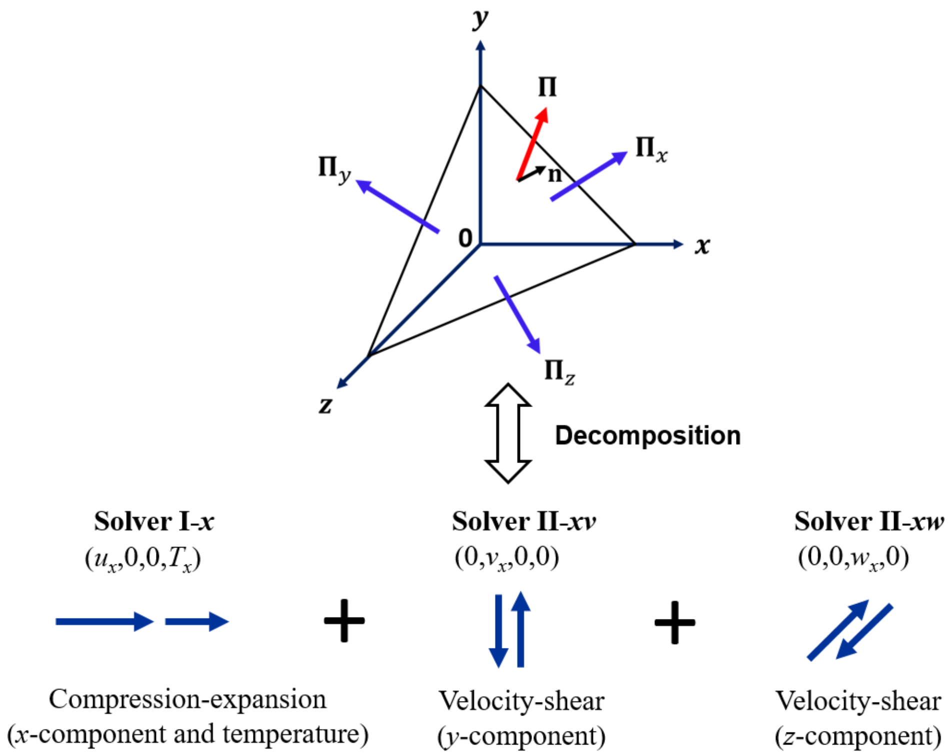

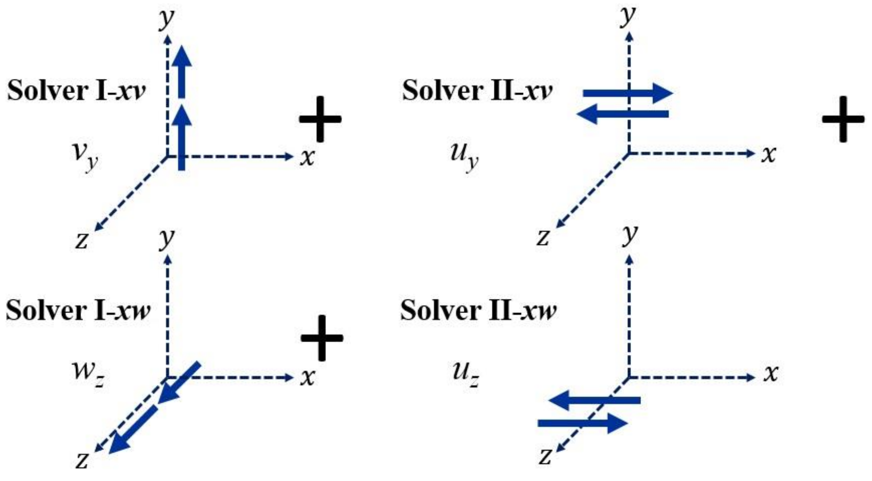

Primary surface integral

Secondary volume integral

Comparison of the NCCR solution with the DSMC

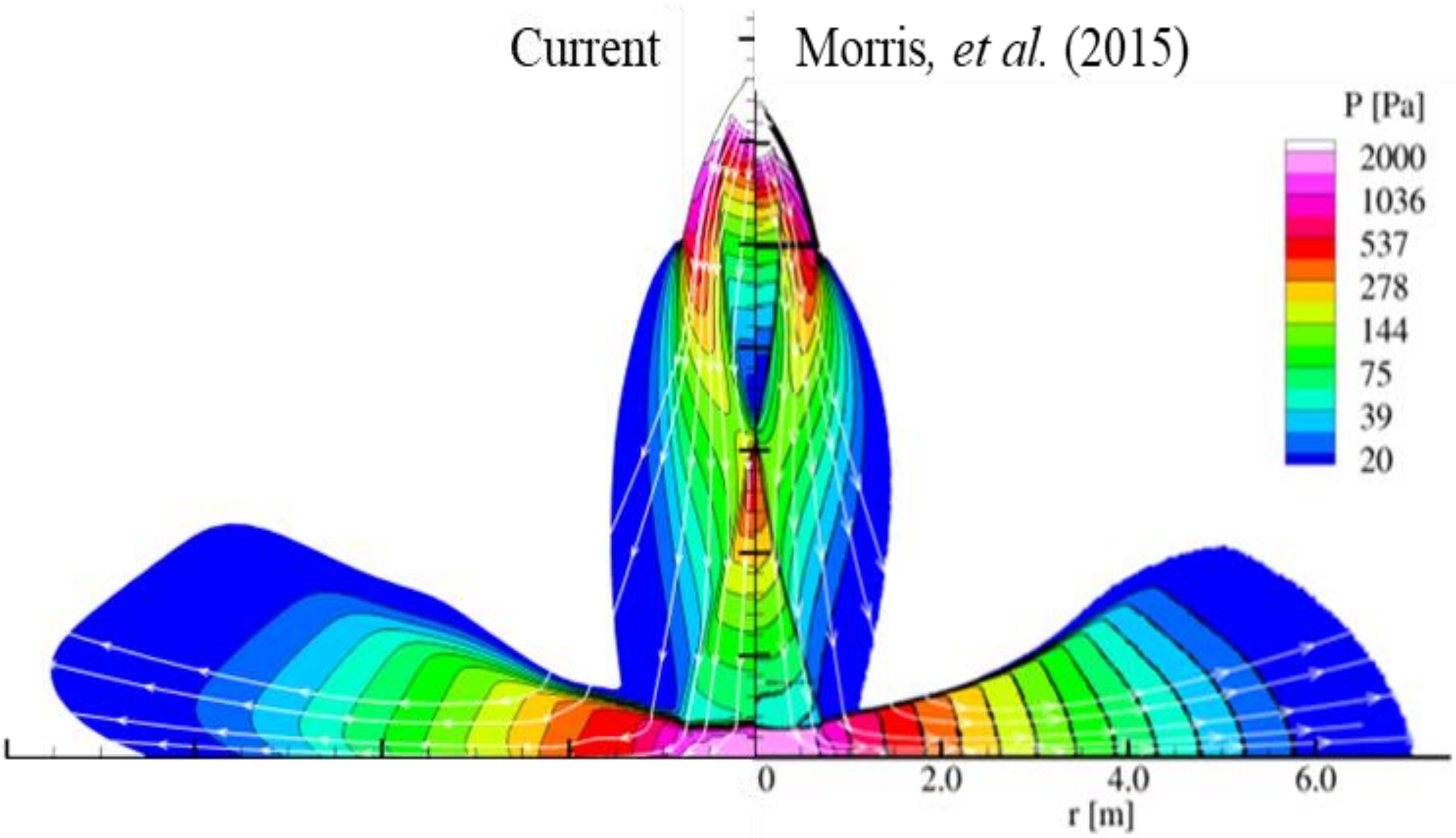

O. Ejtehadi, R. S. Myong, I. Sohn, B. J. Kim, "Full continuum approach for simulating plume-surface interaction in planetary landings," *Physics of Fluids*, Vol. 35, 043331, 2023.

Effects of the ambient pressure on the plume

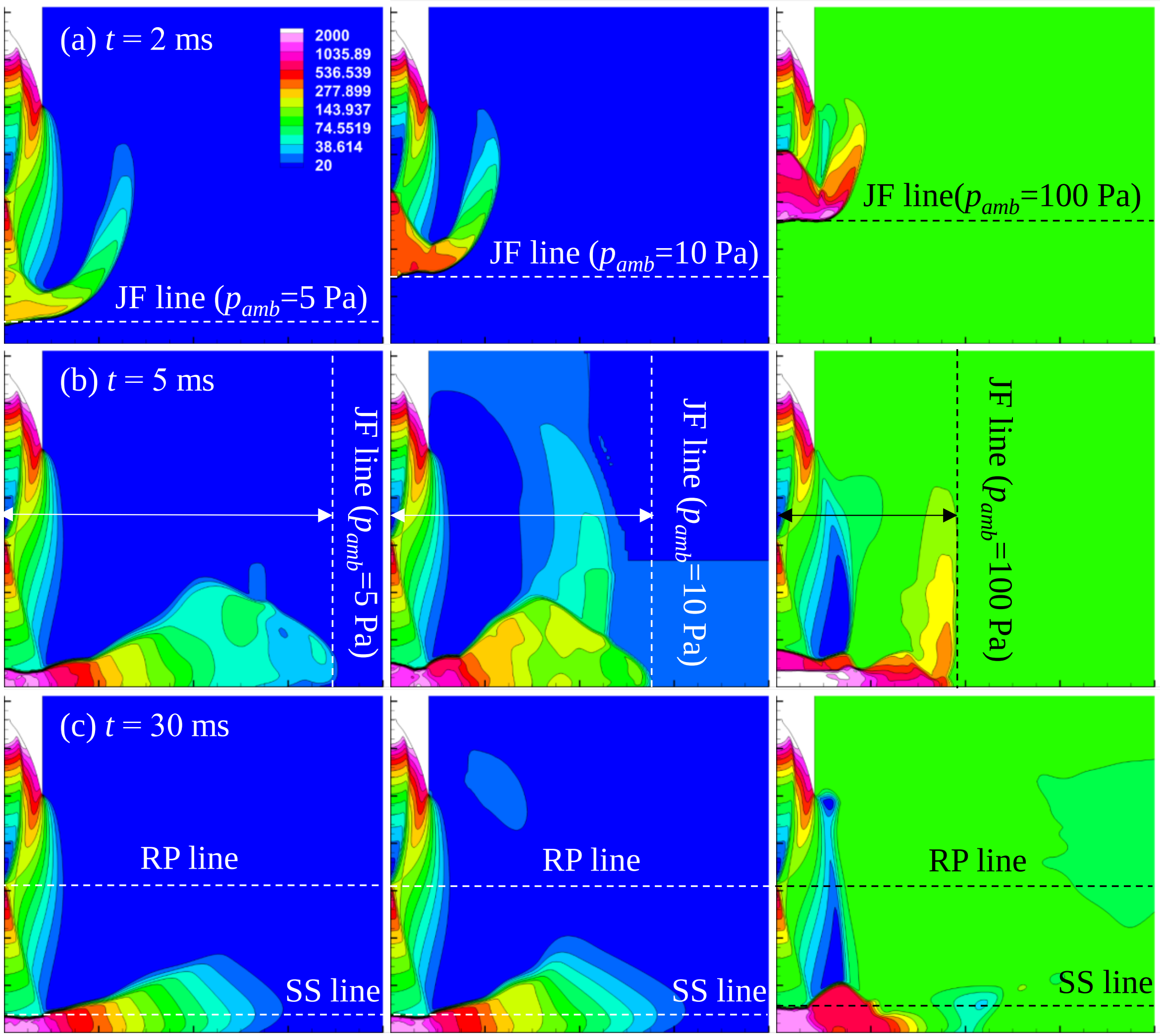

Jet Front (JF)

Reflective Point (RP)

Standoff Shock (SS)

Effects of the height of the dusty bed

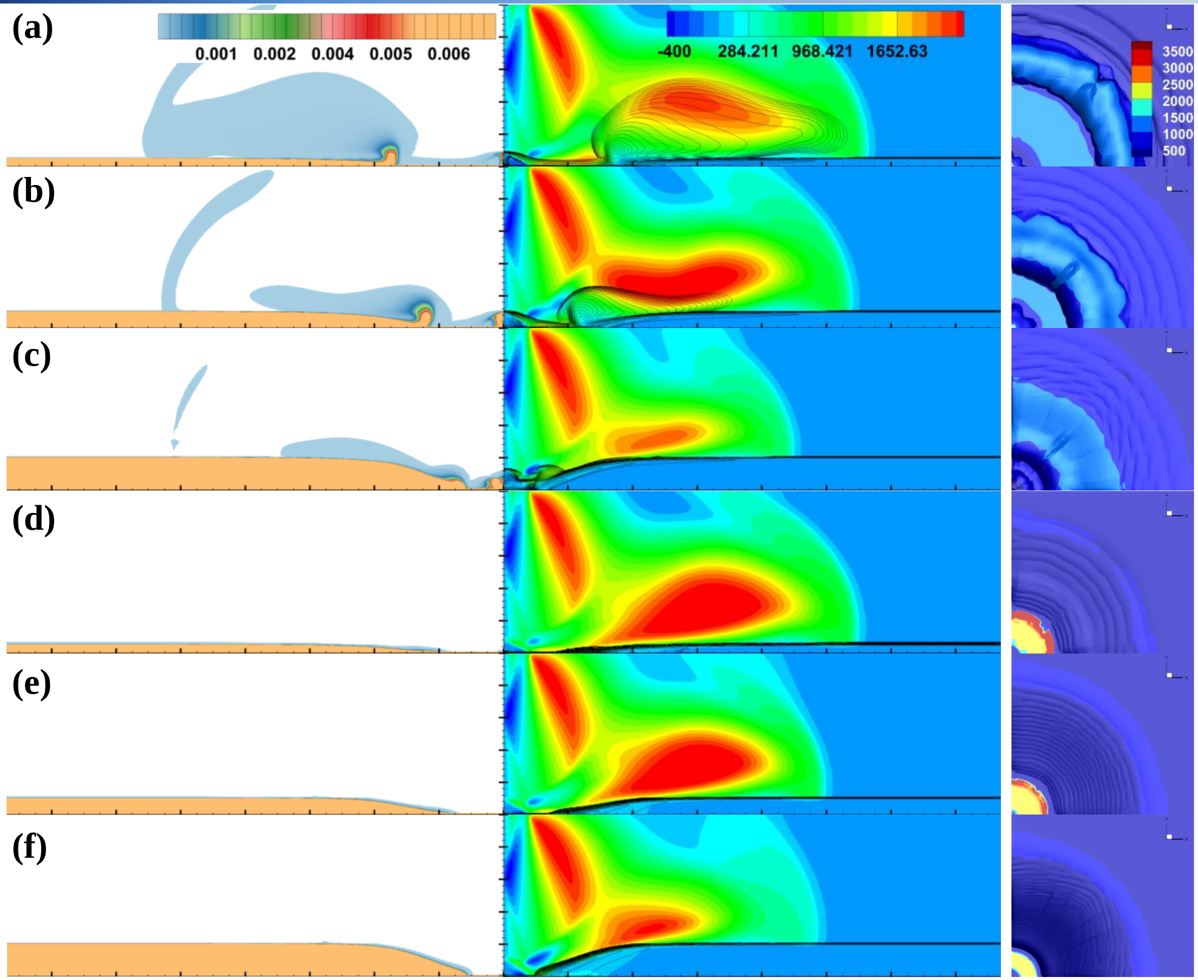

(a)-(c) 5 μm

(d)-(f) 10 μm

Stokes number

$$St = \frac{\rho_s d^2 / 18\mu_g}{\tau_{carrier}}$$

Solid density; radial velocity of gas contours overlaid on solid density lines; top view of solid density

nccrVibFOAM solver for rarefied & microscale flows

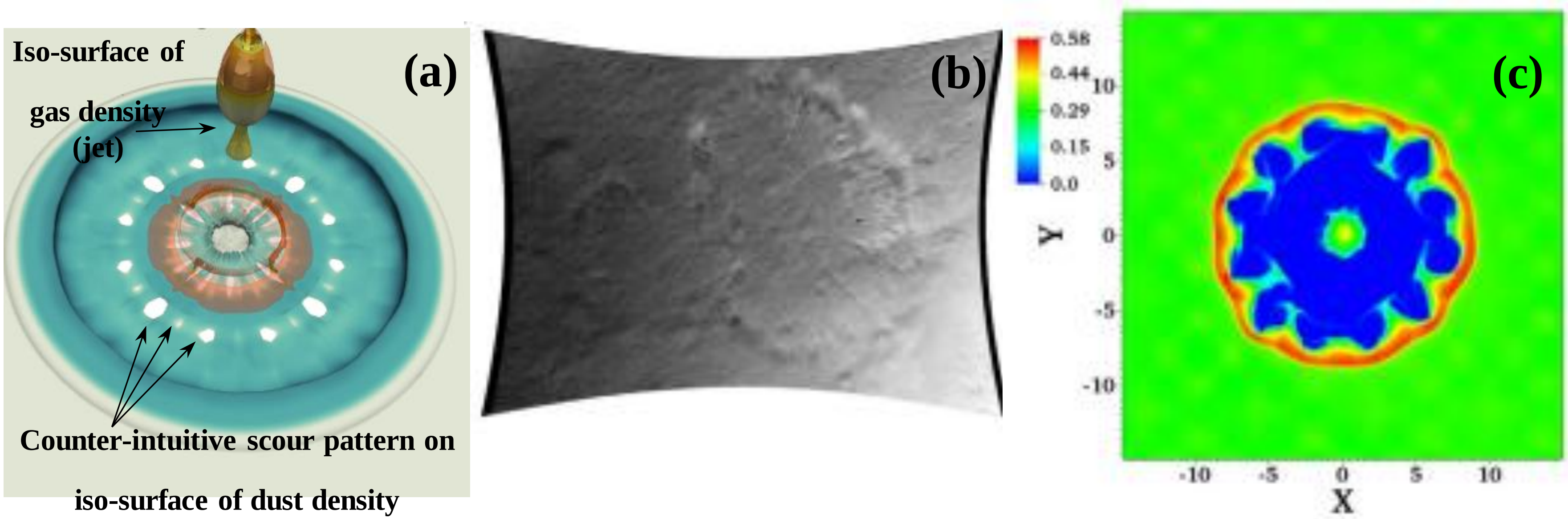

Counter-intuitive non-axisymmetric scour formation during planetary landing: (a) *nccrFOAM* (present); (b) NASA Mars Science Laboratory (MSL) landing image; (c) Simulation conducted in Jet Propulsion Laboratory (K. Balakrishnan and J. Bellan, “High-fidelity modeling and numerical simulation of cratering induced by the interaction of a supersonic jet with a granular bed of solid particles,” Int. J. Multiphase Flow, Vol. 99, 1-29, 2018.)

Other ongoing and future topics

- Needle-free injection where drug particles are delivered by shock waves

  O. Ejtehadi, T. Mankodi, I. Sohn, B. J. Kim, R. S. Myong, " Gas-particle flows in a microscale shock tube and collection efficiency in the jet impingement on a permeable surface," *Physics of Fluids*, Vol. 35, 043331, 2023.

- Shielding IR signals by injecting particles into the engine exhaust plume

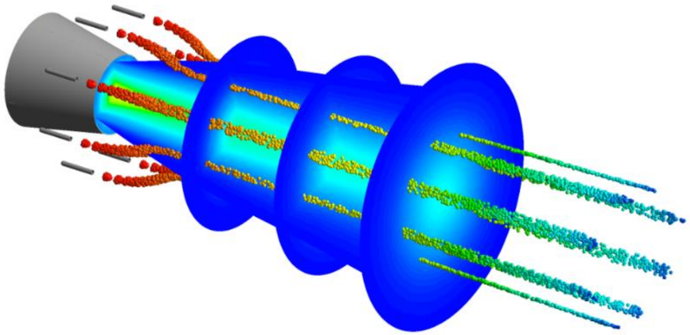

Lee, Y. R., Lee, J. W., Shin, C. M., Kim, J. W., Myong, R. S., "Particle Layer Effects on Flowfield and Infrared Characteristics of Aircraft Exhaust Plume," *Journal of Aircraft*, Vol. 59, No. 5, pp. 1320-1336, 2022.

- Application to multi-rotor configurations (compound, UAM)
- High-lift wing aerodynamics (combination of propellor/rotor/proprotor, wing, and suction/blowing) for hydrogen fuel cell electric aircraft
- Poly-disperse description, inclusion of solid particle collisions, extension to far-field simulation
- From meta modeling to physics-guided AI modeling in case of highly non-equilibrium flow regimes